REPORT NO. FRA-RT-73-21

PB 219 820

ANALYTICAL STUDIES OF THE LIFT AND ROLL STABILITY OF A RAM AIR CUSHION VEHICLE

Timothy M. Barrows

DECEMBER 1972
INTERIM REPORT

Prepared for

DEPARTMENT OF TRANSPORTATION
FEDERAL RAILROAD ADMINISTRATION
Office of Research, Development and Demonstrations
Washington, D.C. 20590

TECHNICAL REPORT STANDARD TITLE PAGE

1. Report No.	2. Government Accession No.	3. Recipient's Catalog No.
FRA-RT-73-21		PB-214 520

4. Title and Subtitle	5. Report Date
ANALYTICAL STUDIES OF THE LIFT AND ROLL STABILITY OF A RAM AIR CUSHION VEHICLE	December 1972
	6. Performing Organization Code
7. Author(s)	8. Performing Organization Report No.
Timothy M. Barrows	DOT-TSC-FRA-72-10
9. Performing Organization Name and Address Department of Transportation Transportation Systems Center Kendall Square Cambridge, MA 02142	10. Work Unit No. R3316 11. Contract or Grant No. RR307
12. Sponsoring Agency Name and Address Department of Transportation Federal Railroad Administration Office of Rsch., Dev. and Demonstrations Washington, D.C. 20590	13. Type of Report and Period Covered Interim Report July 1971 to June 1972 14. Sponsoring Agency Code

15. Supplementary Notes

16. Abstract

A ram air cushion vehicle (a type of ram wing) is described schematically and compared with a conventional air cushion vehicle design. The nonlinear equations for the flow in the cushion region are derived. A review is made of the most recent literature on the subject of wings operating in a rectangular channel, and an approximate solution is developed which shows the relative effects of momentum and viscosity on the pressure distribution. Several analytic solutions are presented which show the effect of a small roll angle on the flow pattern; equations for the rolling moment coefficient are also obtained. It is recommended that future efforts be aimed at developing proper numerical techniques which can solve the nonlinear flow relations and that recent experimental efforts to obtain the lateral stability coefficients be continued and expanded.

March 1973

17. Key Words	18. Distribution Statement
Ram Wing Ram Air Cushion Tracked Air Cushion Vehicle	DOCUMENT IS AVAILABLE TO THE PUBLIC THROUGH THE NATIONAL TECHNICAL INFORMATION SERVICE, SPRINGFIELD, VIRGINIA 22151.

19. Security Classif. (of this report)	20. Security Classif. (of this page)	21. No. of Pages	22. Price
Unclassified	Unclassified	68	$3.00

Form DOT F 1700.7 (8-69)

PREFACE

The work described in this report represents part of an ongoing effort to develop a high speed ground transportation vehicle utilizing aerodynamic forces for suspension. Small scale model demonstrations of this concept were carried out at Princeton University as early as 1965, and low level efforts have continued ever since that time. The Federal Railroad Administration has funded this program for the past four years, through the Office of Research Development, and Demonstrations.

The present document summarizes the most recent theoretical results, while experimental efforts are reported elsewhere. Sufficient promise has been shown by this concept to initiate a system definition study which will define the characteristics of a complete ram air cushion vehicle and guideway. It is anticipated that the results of this study will become available in the summer of 1973.

TABLE OF CONTENTS

LIST OF ILLUSTRATIONS

LIST OF ILLUSTRATIONS (CONTINUED)

LIST OF ABBREVIATIONS AND SYMBOLS

A	Average potential - Eq. (2-7)
A_n	Fourier coefficients - (3-27)
c	Chord length
c^i	Constant
C_d	Drag coefficient-Drag/$\frac{1}{2}\ \rho U_\infty^2 S$
C_L	Lift coefficient-Lift/$\frac{1}{2}\ \rho U_\infty^2 S$
C_p	Pressure coefficient-$(p-p_\infty)/\frac{1}{2}\ \rho U_\infty^2 S$
C_ℓ	Rolling moment coefficient-Roll moment/$\frac{1}{2}\ \rho U_\infty^2 S$
h	Channel height
i	$\sqrt{-1}$
$\vec{i}$	Unit vector in x direction
$\vec{j}$	Unit vector in y direction
k	Constant - Eq. (3-14)
m	Mass flux into channel and out side gaps
p	Pressure
p_∞	Freestream pressure
P	Power required
q	Complex velocity v-iw
Q	Magnitude of velocity - Eq. (2-2)
r	Mass flux ratio δ/α.
s	Semispan (one half width of channel)
	Taken as unity throughout report
S	(Section 2) Planform area
S	(Section 3) Sink function - Eq. (3-32)
t	Time

LIST OF ABBREVIATIONS AND SYMBOLS (CONTINUED)

u_o Steady State x-velocity in channel

u' $u-u_o$

U_∞ Freestream velocity - Taken as unity throughout report

v y-velocity

w Vertical velocity through side gaps

x Longitudinal coordinate

x_T Trailing edge variable - Eq. (2-38)

y Lateral coordinate

y_r Right tip variable y-1

z Vertical coordinate

α Angle of attack

γ (Section 2) $\tan^{-1} r$

γ (Section 3) Roll angle

Γ Circulation

δ Side gap

∇ Gradient - Eq. (3-2)

ε Vertical clearance at trailing edge

ρ Air density

Φ Velocity potential

ϕ Perturbation velocity potential

ϕ^u Potential for unit flux in each half of channel

λ Eq. (2-19)

$\lambda_{1,2}$ Eq. (2-43)

Θ $\cos^{-1} u$

LIST OF ABBREVIATIONS AND SYMBOLS (CONCLUDED)

Subscripts

x,y Derivative w.r.t. x,y

1,2,3 Eq. (3-6)

o Steady state crossflow condition (page 30)

Superscripts

-	Quantity divided by ε
~	Quantity divided by δ
i	Inner solution
c	Channel solution
o	Outer solution
p	Particular solution
h	Homogeneous solution

All lengths are normalized by the semispan. All velocities are normalized by the freestream velocity.

1.0 INTRODUCTION - ADVANTAGES OF A RAM AIR CUSHION

The possibility of using aerodynamic lift to support a high speed ground transportation vehicle has been recognized for some time. A variety of terms have been created to denote this concept, none of which has achieved wide recognition. The original term, ram wing, was coined by Kaario, a Finnish Engineer who actually built a small craft which flew over the ice on a lake in Finland. Although his device did in fact resemble a wing, the studies which have been conducted for the Office of Research, Development, and Demonstration (ORD+D) of the Federal Railroad Administration indicate that the most promising concept for utilizing aerodynamic lift is to simply shape the bottom surface of the vehicle in such a way that with forward speed a high pressure region is created which provides lift. It is somewhat misleading to call the resulting shape a wing, since this implies a structure with relatively large span, whereas in fact no more width is necessary than that required to house the passengers. The vehicle may thus closely resemble current designs for tracked air cushion vehicles, with the major difference being the lack of air compressors. The term "ram air cushion" describes this exactly; an air cushion which is pressurized by ram air.

The advantages to be gained over conventional cushion design go far beyond simply eliminating the weight and power consumption of the compressors. It is the purpose of this first chapter to describe these advantages in some detail; this will lend some insight into the analytic techniques developed in the later chapters. Also, it is important to focus on the differences of this concept relative to conventional air cushion design so that the most promising aspects can be evaluated and future research can focus in these areas.

Previous studies of this concept at TSC have avoided proposing a specific vehicle-guideway cross-section in order to remain open to the greatest number of possible configurations. While this approach has the advantage of generality it does tend to

leave the concept in a rather abstract state and thus makes it hard to evaluate relative to conventional air cushion designs. For this reason the following discussion proposes a ram air cushion which operates in a channel guideway. This configuration not only offers a number of advantages from a dynamic standpoint but it is the chosen guideway for the 300 mph tracked air cushion vehicles currently under investigation by ORD+D and thus may serve as an excellent basis for comparison.

Schematic diagrams of the two concepts appear in Figures 1-1 and 1-2. An essential difference between them is the requirement for at least four separate cushions in the cross-sectional plane for the conventional design, each of which requires a seal or barrier on either side, for a total of eight seals. The fluid in these cushions moves fairly slowly with respect to the vehicle, so that the pressure is uniform, and in order to exert different pressures on different surfaces of the vehicle it is necessary to have distinct cushions with separating barriers between them. This type of design might be called a static air cushion, since the air in the cushion region is essentially static.

One of the principal advantages of the present concept is that the fluid is moving at a substantial velocity relative to the vehicle, and thus pressure differences can be maintained between different locations of the same cushion. Thus when the vehicle moves to the right, for example, the pressure on the right may increase while that on the left decreases, even though no physical barrier separates these regions, and a restoring force is created which centers the vehicle in the guideway. This single dynamic cushion can therefore replace four static cushions, and only two seals are required, one on each side of the vehicle.

For clarity of thought, it should be pointed out that in fact two ideas are involved here; first, to use the ram effect to pressurize the cushion, and second, to allow this air to move at a substantial velocity so that the dynamic effect is obtained. These ideas are quite independent. We could certainly use a compressor to supply air to a dynamic cushion, or we could use ram air to pressurize a static cushion -- a static ram air cushion. Thus what

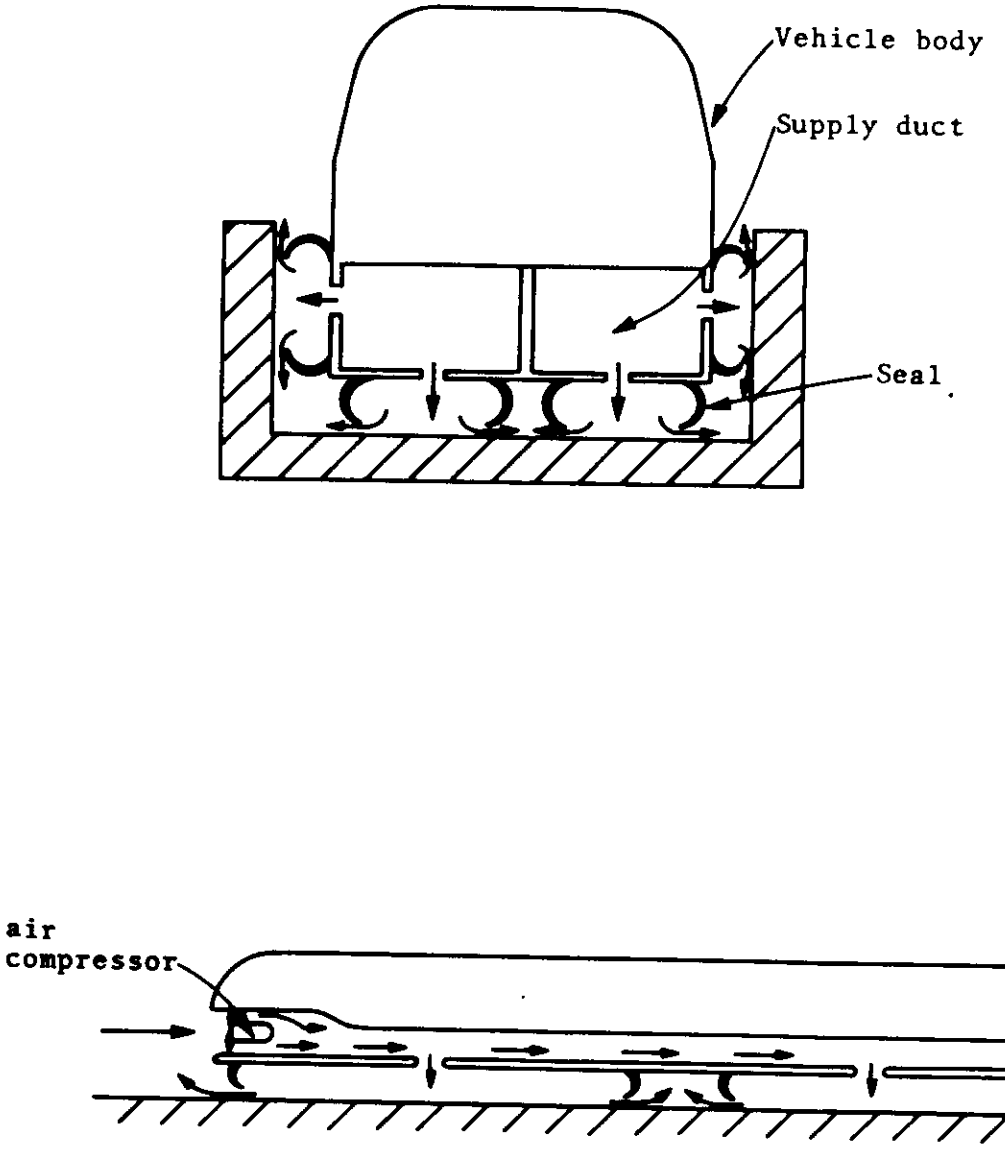

Figure 1-1. Conventional Air Cushion Vehicle

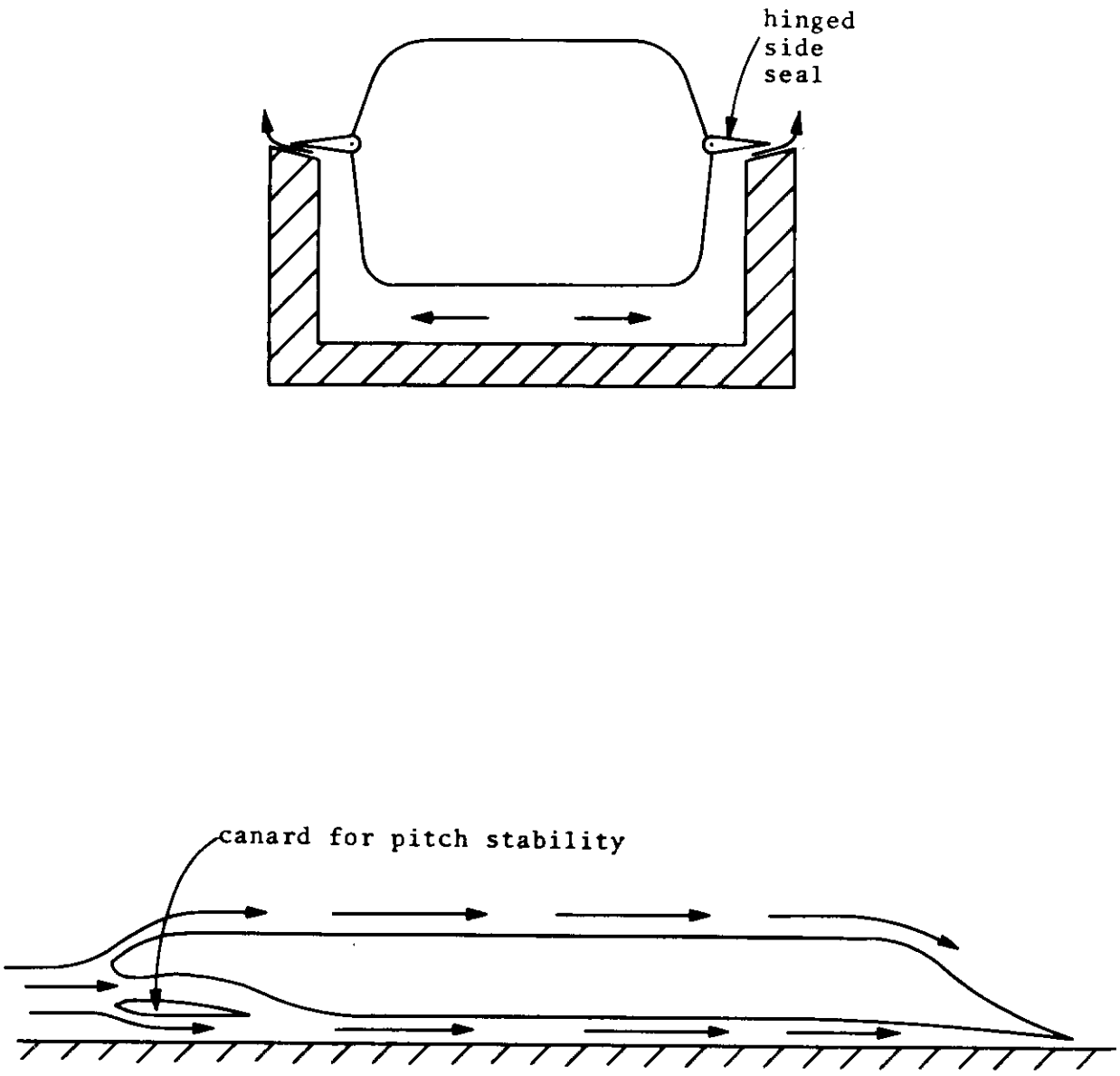

Figure 1-2. Ram Air Cushion Vehicle

we have been calling a "conventional" cushion would be a static pressurized cushion. These ideas are illustrated in Figure 1-3.

The previous discussion has emphasized the number of seals associated with each design, even though one might not at first suspect that this is a particularly significant item. However, it should be pointed out that these seals all must come in close proximity to the guideway, and if they are not to be worn away rather rapidly the guideway surface tolerances must be very stringent, which can greatly increase the capital and maintenance costs of the system. Static cushion design dictates that seals be placed at the front and rear of each cushion, so that the entire guideway surface must be smooth and carefully aligned, this is particularly difficult in the case of transition spirals leading into turns which must be curved and twisted rather precisely. It is apparent after some reflection that if the tolerance requirements can be limited to the specific paths which the side seals follow as the vehicle travels, the alignment problem is greatly simplified. One could construct a guideway whose surface conformed to ordinary highway standards and then finish these narrow paths to within any desired tolerance. As another alternative, it has been proposed by Giraud (1969) that light adjustable steel rails be built along the paths which each of the eight side seals follow as the vehicle travels. This "adjustable lips path" would allow a smooth ride and low lip wear on a guideway with poor surface quality, and the vehicle path could be realigned within limits without moving the entire guideway. The dynamic cushion concept makes this doubly attractive since only two seals, and hence only two adjustable paths, would be required, reducing the cost of these rails by 75 percent.

A major deficiency of a static air cushion design is its excessive power consumption. There are two major reasons for this: control power and captation drag. Control power is required in order that a cushion may have the capability to develop a force greater than its nominal force level when it is displaced toward the guideway surface. Typically, the pressure in the supply ducts is 50 percent higher than the cushion pressure. This pressure

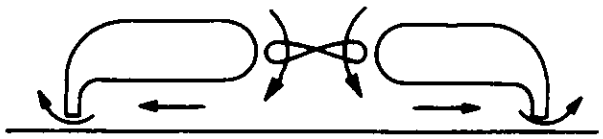

Static Pressurized Cushion

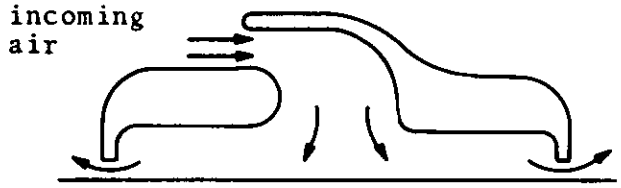

Static Ram Air Cushion

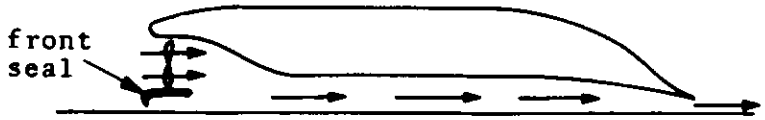

Dynamic Pressurized Cushion

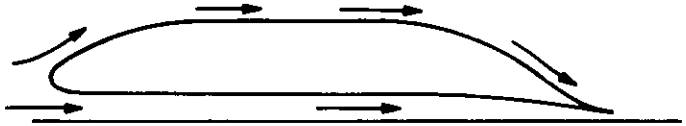

Dynamic Ram Air Cushion

Figure 1-3. Classification of Fluid Suspension Concepts

difference is maintained by one or more small orifices through which the fluid passes as it enters the cushion. When the cushion is "bottomed out", the airflow and hence the pressure drop across these orifices become zero, the plenum pressure rises to the supply pressure and the total lift force reaches its maximum. At the nominal operating condition the cushion continually uses excess power at a rate equal to the pressure drop across the orifice times the flow rate in order to maintain this extra force capability.

With the dynamic air cushion the potential for control forces is contained in the kinetic energy of the fluid. The cushion geometry must be arranged such that as its periphery is displaced toward the guideway surface, the fluid velocity is decreased and the pressure increases. An important point is that at the nominal condition no excess power must be consumed since the kinetic energy of the fluid is naturally present if the vehicle is moving at a high forward speed. The energy for the extra force is only used when necessary and is reflected in a slight increase in vehicle drag at times of high cushion pressure. At times of low pressure the drag decreases so that on the average no net energy is consumed due to control requirements.

An even more serious power penalty associated with the static air cushion is the captation drag, also known as ram drag. Since the fluid has little rearward velocity relative to the vehicle, as it leaves the cushion it has the same velocity as the vehicle relative to the external atmosphere. Thus, the cushion continually trails a wake of forward moving air, rather like a jet engine with its thrust reverser permanently on. This causes an unseemly amount of noise and power consumption, with the resulting drag force increasing linearly with forward speed. As an illustration, the tracked air cushion research vehicle (TACRV) built for ORD+D has a captation drag at 300 mph of 3000 lbs. Previous design efforts to minimize this loss have focused on the compressor inlet, but these have had very limited success, since it is essential to deal

with the point where the flow leaves the cushion. The obvious solution to this problem is to allow the air in the cushion to exit with a rearward velocity relative to the vehicle, which is precisely what is done with a dynamic air cushion.

A further advantage of dynamic operation is that active suspension control is far more convenient. The static air cushion requires some kind of fast control valve which can alter the flow into the plenum region, or else an active secondary suspension, which generally implies a separate hydraulic or pneumatic system. In contrast, the large flux of fluid through the dynamic cushion means that a small change in the flow conditions at the trailing edge (using either a mechanical or a jet flap) can produce a huge change in the resulting force. Thus, control forces can be generated quickly and easily by whatever logic device may be employed.

At this point, it should be evident that static air cushions are not ideally suited to the task of suspending a high speed vehicle. Their performance represents the lower bound of what can be obtained from a fluid suspension system. Conventional designs go to a huge effort and expend vast amounts of energy to eliminate something which is very valuable: the incoming momentum of the air. As a number of advantages can be claimed for preserving this momentum and no disadvantages are apparent, there appears to be little room for argument against incorporating at least some dynamic features into the cushion, even though the precise details of how best to do this may remain unclear. On the other hand, the complimentary concept of using ram air to pressurized the cushion involves one disadvantage: some alternative method of suspension is required for low speeds. This deserves some further comment.

There are several arguments in favor of combining the two concepts that tend to outweigh the relatively minor difficulty associated with landing gear. A ram air cushion vehicle can operate at a vehicle clearance which is only limited by the height of the guideway sidewalls. Clearances on the order of one foot mean that small obstacles and debris do not pose a serious threat, and

the requirement for a secondary suspension can be eliminated since the vehicle can move up and down through a substantial range. Also, high speed transfer of vehicles from one lane to another may be accomplished very conveniently. This is one aspect of high speed ground transportation which has heretofore received relatively little attention but is very important since it defines the line capacity of the system. High capacity dictates a passive switch which does not require any moving parts on the guideway. The importance of this problem is underscored by the recent decision of Tracked Hovercraft Limited to change their guideway from a simple box beam to a wider track which provides roll stability from the levitation surface. They have concluded that lateral guidance should be provided by magnetic forces, the major impetus behind these changes being the necessity of a convenient switching scheme. However, the unique ability of a ram air cushion to operate with unlimited vertical clearance can be exploited in a number of ways to vertically switch the vehicle into either of two branches of the guideway. This is one of the few switching concepts which meets all of the requirements of a high speed system.

A substantial reduction of the frontal area of the vehicle can be obtained since no supply ducts are required for the cushion. It is extremely important that this area be minimized since the aerodynamic drag represents by far the largest single component of the total power requirement. The elimination of these ducts means the entire profile of the vehicle is lowered, resulting in better dynamics (from the lower center of gravity) and less disturbance due to crosswinds and passing oncoming vehicles in adjacent lanes. Furthermore, the small orfices which lead from the ducts into the individual cushions on a conventional design tend to become clogged with leaves and other debris; the ram air cushion obviously does not suffer this problem since there are no ducts or orifices.

Finally, there is the most obvious advantage; eliminating the noise, weight, and power consumption of the air compressors. These benefits do not accrue without a cost, represented by the wheels which must be used at low speeds, although the example of the airline industry can be used to demonstrate that landing gear certainly does not constitute an obstacle to commercial success, and it is obvious that the operating requirements of aircraft landing are far more severe than anything expected for an HSGT system. Furthermore, the wheels themselves can be used to great advantage in certain situations (power failures and tight turns at low speeds) so that on the whole the benefits appear to heavily outweigh the costs. However, since virtually all of the research effort at TSC was devoted to analyzing the dynamic aspects of the cushion, no further discussion is warranted on the concepts of using the ram effect for pressurization, and we may turn to the calculation of the forces, moments, and stability derivatives of vehicles utilizing aerodynamic suspension.

2.0 SOLUTIONS FOR SYMMETRICAL FLOW

This report is a sequel to the work conducted at TSC by Barrows (1971), which is hereafter referred to by (A). There the case of a lifting surface in a rectangular trough, Figure 2-1, is analyzed in some detail, and it is shown that the lift is composed of two parts. This idea is so fundamental to all of the developments in the present report that it deserves a careful review and some additional physical explanation.

The first component of lift is associated with the inertia of the fluid, and is called the momentum lift. It is proportional to the angle of attack α, very much of the same nature as the lift from a conventional airplane wing. The second component is due to the effect of viscosity at the side edges, this gives rise to a "vertical drag" which is proportional to the square of α (for $\alpha<<1$). For lack of a better term, this will be called the cushion lift, since it may be analyzed in the same manner as the lift from a plenum air cushion.

The relative importance of these two components may be determined from the aspect ratio of the lifting surface. A wing of large aspect ratio will generate almost all of its lift from the momentum effect, whereas for a lifting surface of small aspect ratio the cushion lift will predominate. However, for a proper understanding of the stability derivatives of a ram air cushion a knowledge of both components of lift is essential.

It is very useful to apply the notion of slender body theory to the problem of Fig. 2-1. Imagine a thin slice of fluid encompassing a crossflow plane in a stationary frame of reference, so that an unsteady motion occurs as the plate moves forward. We obtain the picture shown in Figure 2-2, in which the plate starts at the height of the leading edge and moves downward to the height of the trailing edge. Because of inertia, at the initiation of the motion the fluid offers resistance to the acceleration required to pass out the side edges, thus giving rise

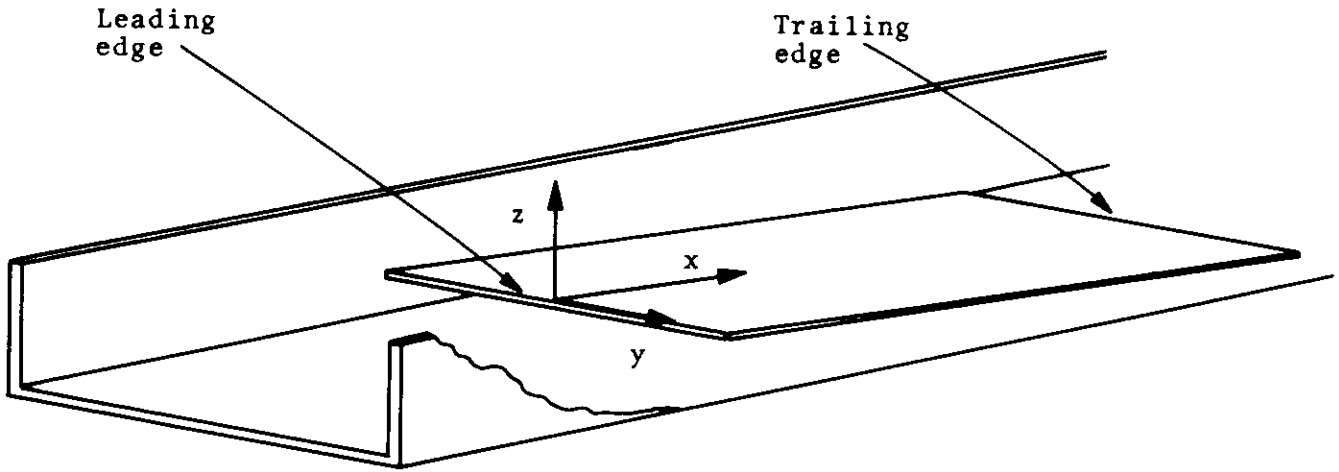

Figure 2-1. Flat Plate in a Rectangular Guideway

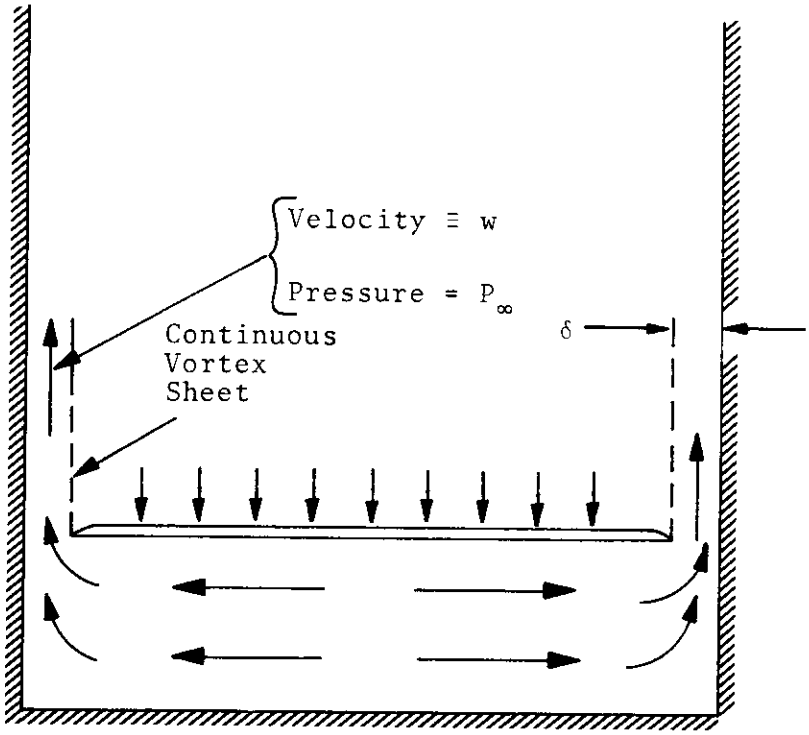

Figure 2-2. Crossplane Flow for the Steady State Component of Motion

to the momentum lift. At a later time, corresponding to the central portion of the plate, the cross plane flow is established in a more or less steady state, but there is still a pressure difference between the upper and lower surfaces due to the separation of the flow off the side edge. The association of the resulting cushion lift with the notion of a vertical drag should be apparent from this picture.

2.1 THE MOMENTUM EQUATION

The Bernoulli equation for incompressible flow with a free-stream velocity of unity may be written

$$\frac{p-p_\infty}{\rho} = \frac{1-Q^2}{2} + \frac{\partial \phi}{\partial t} \qquad (2\text{-}1)$$

where

$$Q^2 \equiv u^2 + v^2 + w^2 \qquad (2\text{-}2)$$

and the subscript ∞ denotes freestream conditions. A velocity potential for the two-dimensional flow pattern shown in Fig. 2-3 has been calculated in (A). This pattern is obviously unrealistic for the steady flow case but should be quite accurate for unsteady motion and thus is useful for calculating the importance of the term $\partial \phi/\partial t$ in (2-1). It may be helpful to note that this is the pattern that acoustic motions would exhibit, even in the presence of a shear layer, which gives us confidence that it is the correct representation of the unsteady component of the flow. The unit solution for the potential at the surface of the wing (z=0) is reproduced here from equation (23) of the above reference:

$$\phi^u = \frac{y^2-1}{2\varepsilon} - \frac{2}{\pi} \ln \frac{4\varepsilon}{\pi^2 \delta^2} \qquad (2\text{-}3)$$

where ε and δ are defined in Figure 2-3. Note that all lengths are normalized by dividing by the semispan. Equation (2-3) is the solution for a downwash flow of one, so that the volume flux m into each half of the channel region is unity. The actual potential as a function of time may be written by allowing for

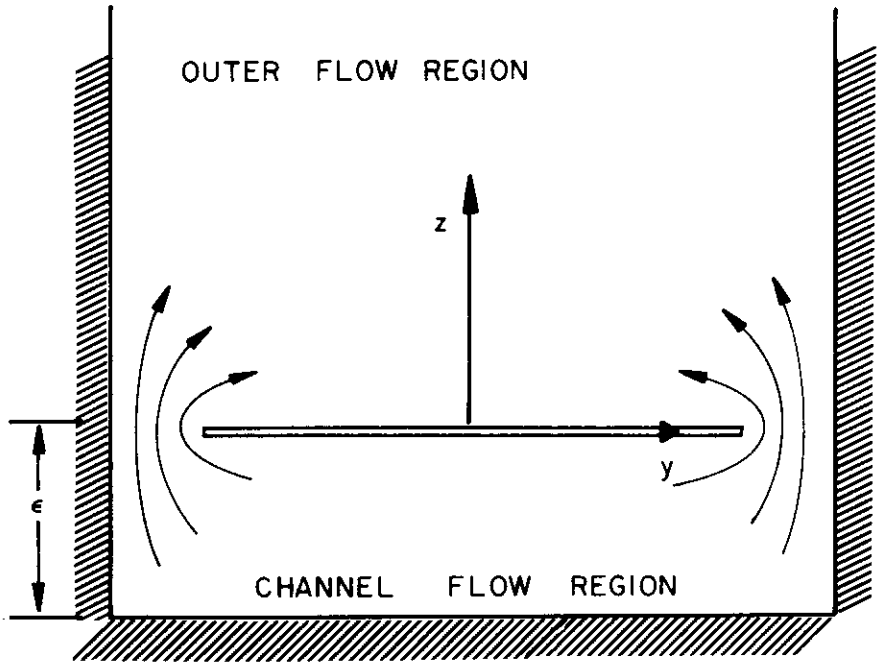

Figure 2-3. Crossplane Flow for the Unsteady Component of Motion

a variable amount of volume flux:

$$\phi(y,t) = m(t)\phi^u(y) \qquad (2\text{-}4)$$

Equating the flux moving into the channel with that exiting out the sides, we have

$$m = \delta w \qquad (2\text{-}5)$$

where w is the average vertical velocity in the side gaps.

The greatest interest in this type of lifting surface lies in the case for which the side gaps are very much smaller than the vertical clearance:

$$\delta \ll \varepsilon \qquad (2\text{-}6)$$

In this situation the variations in the flow conditions across the span assume a secondary importance compared to potential difference above and below the wing, and it becomes very useful to replace the function given in (2-3) by an average value A:

$$A \equiv -\frac{1}{2}\int_{-1}^{+1} \phi^u(y)\,dy \,, \qquad (2\text{-}7)$$

$$= \frac{1}{3\varepsilon} + \frac{2}{\pi}\ln\frac{4\varepsilon}{\pi^2\delta^2}$$

which makes it possible to write

$$\phi(t) = -m(t)A \qquad (2\text{-}8)$$

In this manner a solution is obtained which gives the correct average value at each instant of time, and the problem is greatly simplified since all the variables become functions of time only. By using (2-5) and differentiating, we have

$$\frac{\partial \phi}{\partial t} = -\delta A \frac{dw}{dt} \qquad (2\text{-}9)$$

We now insert this into (2-1), and convert to a coordinate system moving with the plate, so that d/dt is replaced by d/dx. In view of (2-6), v is very small, so that v^2 may safely be neglected in (2-2), which is also substituted into (2-1):

$$\frac{p-p_\infty}{\rho} = \frac{1-u^2-w^2}{2} - \delta A\frac{dw}{dx} \qquad (2\text{-}10)$$

It is implicitly assumed that the u velocity is uniform at each station. This equation is applicable to the free streamline which emanates from the edge of the plate as in Fig. 2-2. It is a property of such streamlines that the pressure on each side must be the same, which means that p must be approximately equal to p_∞, and both sides of (2-10) may be equated to zero. The result is best written in the form of a differential equation for the velocity in the side gap:

$$\frac{dw}{dx} = \frac{1-u^2-w^2}{2\delta A} \qquad (2\text{-}11)$$

In the channel region, where the vertical velocity is very small, the pressure coefficient may be written

$$C_p = \frac{2(p-p_\infty)}{\rho} = 1-u^2 \qquad (2\text{-}12)$$

Using this in (2-11), we have

$$C_p = 2\delta A\frac{dw}{dx} + w^2 \qquad (2\text{-}13)$$

This relation explicitly shows the contributions to the momentum lift and the cushion lift, respectively. For small δ one would expect the cushion lift to predominate, except for those regions in which w is very small. It should be clear from the slender body analysis that w=0 at the leading edge of the wing; thus for any values of the parameters δ and ε, the momentum lift will predominate there.

2.2 THE CONTINUITY EQUATION AND BOUNDARY CONDITIONS

A side view of the plate in a trough is shown in Figure 2-4. The height of the channel is given by

$$h(x) = \varepsilon+\alpha(c-x) \tag{2-14}$$

and the variation in volume flux through the channel is equal to the flux out the sides calculated previously:

$$\frac{d(hu)}{dx} = -\delta w \tag{2-15}$$

Substituting from (2-14), and reproducing (2-11), we obtain a set of equations for u and w:

$$\frac{du}{dx} = \frac{\alpha u-\delta w}{h(x)} \tag{2-16a}$$

$$\frac{dw}{dx} = \frac{1-u^2-w^2}{2\delta A} \tag{2-16b}$$

At the trailing edge the kutta condition states that the pressure coefficient is zero, which gives a boundary condition on u using (2-12). This together with the leading edge condition gives a well-defined problem:

$$w=0 \text{ at } x=0 \tag{2-17a}$$

$$u=1 \text{ at } x=c \tag{2-17b}$$

Although these equations could in principal be solved numerically, there are certain pitfalls associated with this type of non-linear two-point boundary value problem, and it is very worthwhile to review some of the previous efforts of various investigators. All these efforts have ignored one or more terms of (2-16), and thus provide interesting limiting cases against which the more accurate solutions developed herein may be checked.

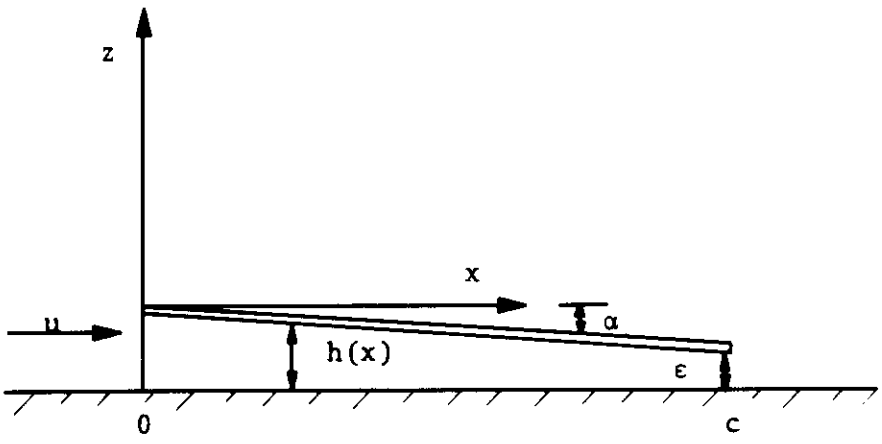

Figure 2-4. Side View of the Flat Plate of Figure 2-1

2.3 CASE I - LINEARIZED POTENTIAL FLOW THEORY

This case has been investigated in (A) and is reproduced here in a slightly different form which lends some additional insight. There it was shown that as the chord c of the wing becomes infinite, the total momentum lift approached a finite asymptotic value. This means that for wings of very low aspect ratio the after portion of the wing has a negligible effect on the flow pattern, so that from a mathematical standpoint we may let $c \to \infty$ and the calculated pressure distribution varies little from the case of $c >> 1$. Since the solution assumes a simplified form in this case it becomes very useful when more complex real fluid effects are included.

A necessary condition for linearized flow (Widnall and Barrows, 1969) is that

$$\alpha >> \varepsilon \tag{2-18}$$

which means

$$h \tilde{=} \varepsilon$$

We introduce several new parameters which simplify the analysis of the problem

$$\begin{aligned} \bar{\alpha} &\equiv \alpha/\varepsilon \\ \bar{\delta} &\equiv \delta/\varepsilon \\ \lambda^2 &\equiv 1/A\varepsilon \end{aligned} \tag{2-19}$$

The governing equations become

$$w_x = \frac{\lambda^2}{2\bar{\delta}} (1-u^2-w^2) \tag{2-20}$$

$$u_x = \bar{\alpha}u - \bar{\delta}w \tag{2-21}$$

A perturbation potential ϕ is introduced in the usual fashion, such that

$$\begin{aligned} u &= 1 + \phi_x \\ u^2 &= 1 + 2\,\phi_x + \phi_x^2 \end{aligned} \tag{2-22}$$

This is substituted into (2-20), and the terms w^2 and ϕ_x^2 are neglected since they are squared quantities, yielding

$$w_x = -\lambda^2 \phi_x/\bar{\delta}$$

Integrating and rearranging:

$$\bar{\delta} w = -\lambda^2 \phi$$

Upon inserting this into (2-21) and observing that $u \tilde{=} 1$, we obtain

$$\phi_{xx} - \lambda^2 \phi = \bar{\alpha} \tag{2-23}$$

The boundary conditions for the case of infinite chord become

$$\phi = 0 \quad \text{at} \quad x=0$$
$$\phi_x = 0 \quad \text{at} \quad x=\infty$$

and the solution is simply

$$\phi = \frac{\bar{\alpha}}{\lambda^2} (e^{-\lambda x} - 1) \tag{2-24}$$

From this we may obtain the pressure coefficient

$$C_p = -2\phi_x = \frac{2\bar{\alpha}}{\lambda} e^{-\lambda x} \tag{2-25}$$

This gives the average pressure across the span, which is sufficient for calculating lift and moment coefficients. If the spanwise pressure distribution is required it may be obtained by generating weighting factors using (2-3).

A useful formula for the lift on a long plate may be written as follows:

$$C_{L_S} = -\phi(\infty) = \frac{\bar{\alpha}}{\lambda^2} \tag{2-26}$$

where C_{L_S} is the lift coefficient based on the square of the span.

The solution given by (2-24) involves many simplifying assumptions but for a wing of large chord it should certainly be adequate to calculate the momentum lift, which generally amounts to a small portion of the total lift. It should be pointed out that numerical lifting surface schemes using a distribution of horseshoe vortices, such as those given by Gray (1971) and Davis (1972), will merely produce finer and finer approximations to this small component and become increasingly difficult and expensive to implement properly as the parameters ε and δ become small. Such efforts are not warranted until a greater understanding is obtained of the unique aspects of this type of lifting surface.

One observation which can be made is that in spite of the simplicity of (2-23) it is very difficult to numerically compute a solution which satisfies the boundary conditions. A spurious solution exists which diverges exponentially with x, and although with sufficient precision one can suppress this when the chord c is finite, as $c \to \infty$ it becomes increasingly difficult to do so. Although this is not a problem with closed form solutions, any attempt to numerically solve the complete equations (2-16) must resolve this difficulty.

2.4 CASE II - STEADY STATE CROSS-PLANE FLOW

A very interesting solution for the flow under a ram wing has been proposed by Gallington, et. al. (1972). They present a crossplane flow as in Fig. 2-2, and simply treat this flow as uniform from the leading edge to the trailing edge, thus ignoring all derivatives with respect to x. If we set both of these derivatives equal to zero in equations (2-16), we obtain a simple set of algebraic equations:

$$1-u^2-w^2 = 0$$

$$\alpha u-\delta w=0$$

Using (2-12), we obtain

$$C_p = \frac{\alpha^2}{\alpha^2 + \delta^2} \qquad (2\text{-}27)$$

which is equivalent to their solution. They recognized that this simple result was not adequate to explain the flow at the leading edge, and also pointed out the necessity of some kind of flap or constriction at the trailing edge to maintain the elevated pressure there. Nevertheless, their solution is important since it is the first to recognize the profound effect of flow separation off the side edges of the wing.

Several observations can be made immediately. The pressure is uniform under the entire wing and thus the aerodynamic center is at the mid chord. When $\alpha \ll \delta$, this component of flow is proportional to the square of α, but for large α, the pressure coefficient approaches unity, and a stagnation region is formed under the entire wing. At any value of α the pressure is independent of the vertical clearance ϵ, so there is no height stability. With a given span, there is no limit to the amount of lift which can be derived as the chord of the plate is increased, a feature which is in marked contrast to the potential flow solution of Case I. This component of the lift ignores momentum effects and is computed in essentially the same way as the lift from a plenum air cushion, and so it is logical to call this the cushion lift.

The simplest way to arrive at a solution for the total lift is to simply add the two components, as was done in (A) with some success. Although this is admittedly an inaccurate approach, particularly for the moment coefficient, it is a useful concept for the section which follows.

2.4.1 Power Requirements

The drag corresponding to the cushion lift has been obtained by the above authors from the momentum defect of the flow out the side edges. They quite logically call this the momentum drag, although for purposes of this report this term is not used to

avoid association with the momentum lift. We say that the momentum lift causes induced drag, according to aeronautical terminology, and the drag due to cushion lift is called ram drag, the term used in air cushion work.

Their result for the ram drag term, using our present notation, is

$$C_d = 2\delta\ C_L^{1/2}\ [1-(1-C_L)^{1/2}]. \qquad (2\text{-}28)$$

Assuming that $\alpha << \delta$, C_L is very small and

$$(1-C_L)^{1/2} \tilde{=} 1-C_L/2.$$

Thus (2-28) becomes

$$C_d = \delta C_L^{3/2} \qquad (2\text{-}29)$$

Using (2-27) and the above assumption, we have

$$C_L^{1/2} \tilde{=} \alpha/\delta,$$

so that

$$C_d \tilde{=} \alpha C_L \ . \qquad (2\text{-}30)$$

It is thus seen that the net force obtained from a vector sum of the lift and drag acts in a direction which is normal to the plate, very much in the manner of supersonic flow. In other words, for small α the leading edge suction is negligable. It is indeed fortunate that the lift curve slope of this wing is extremely high, so that α is consequently very small and good performance in terms of L/D can be achieved. For large values of α, it should be noted that the drag is considerably less than that given by (2-30).

The power required may be computed from the product of the drag and the velocity. This becomes

$$P = C'\delta' \left[\frac{8}{\rho}\right]^{1/2} \left[\frac{W}{S}\right]^{3/2} \qquad (2\text{-}31)$$

where δ' = dimensional side edge clearance
C' = dimensional chord length
W = vehicle weight
S = planform area

This is essentially the same as the power required to support a given weight with a stationary plenum air cushion of the same planform. However, for the ram air cushion this power is independent of forward velocity, whereas for the pressurized plenum an addition power requirement due to the captation drag must be added.

If the momentum lift is a significant part of the total weight, then the induced drag for this component must be added as part of the total drag due to lift. This can be computed using the method of Barrows and Widnall (1970).

Two cautionary notes must be sounded, however. The total picture for the lift is more complicated than the simple notion used here, and in any case, the formulas in this section are only valid for very small α. These should only be used for comparative purposes, and to show that the power required for lift is very small compared to the power required to overcome parasite drag.

2.5 CASE III - MODIFIED CUSHION THEORY

A recent improvement on the Cushion Theory which eliminates the requirement for a constriction near the trailing edge has been given by Boccadoro (1972). He allows for a variation of u with x but continues to ignore the momentum term w_x in (2-16b), which becomes

$$w = (1-u^2)^{1/2} \tag{2-32}$$

This is substituted into (2-16a), and the boundary condition at the leading edge is ignored:

$$\frac{du}{dx} = \frac{\alpha u - (1-u^2)^{1/2}}{h} , \tag{2-33}$$

$$u = 1 \text{ at } x = c \tag{2-17b}$$

Boccadoro chose to solve this numerically, which is certainly a straightforward matter. However, it is of some interest that an analytic solution is possible, which is given here for the purpose of showing the form of the result. We rearrange (2-33), integrate, and set both sides equal to the same integral I:

$$I = \int \frac{du}{u - r(1-u^2)^{1/2}} = \int \frac{\alpha dx}{h} \quad , \qquad (2\text{-}34)$$

where $r \equiv \delta/\alpha$. Several trigonometric substitutions are required for the first integration.

Let

$$\theta \equiv \cos^{-1} u$$
$$\gamma \equiv \tan^{-1} r$$

We obtain

$$I = -\cos\gamma \int \frac{\sin\theta \, d\theta}{\cos\gamma\cos\theta - \sin\gamma\sin\theta}$$

Now let $t \equiv \theta + \gamma$. This yields

$$I = -\cos\gamma \int \frac{\sin(t-\gamma) \, dt}{\cos t}$$

which is readily integrated:

$$I = \cos^2\gamma (rt + \log \cos t). \qquad (2\text{-}35)$$

The second integral in (2-34) is a simple matter. We use $\alpha \equiv -dh/dx$, giving

$$I = -\int \frac{dh}{h} = -\log h + \text{const.}$$

Rather than equate the two values of I directly, we compute e^{-I} from (2-35) and (2-36) and equate these:

$$h = K \left[\frac{e^{-rt}}{\cos t}\right]^{\cos^2\gamma} \tag{2-36}$$

The multiplicative constant K must be chosen to satisfy the boundary condition, which in our present variables amounts to

$$h = \varepsilon \quad \text{at} \quad \theta = 0$$

We obtain, after some reduction

$$\frac{h}{\varepsilon} = \left[\frac{e^{-r\theta}}{\cos\theta - r\sin\theta}\right]^{1/(1+r^2)} \tag{2-37}$$

As x is directly related to h, and $C_p = \sin^2\theta$, this equation gives an inverse relation between the pressure coefficient and x. Since the boundary condition occurs at the trailing edge of the wing, it is useful to convert to a trailing edge variable x_T which starts at x=c and runs forward:

$$x_T = c - x \tag{2-38}$$

Using (2-14)

$$h = \varepsilon + \alpha x_T \tag{2-39}$$

It is most convenient in using (2-37) to choose several values of θ and then plot the resulting values of C_p and x_T directly, rather than going through the intermediate step of computing u. The result is shown in Figure 2-5. Also shown is C_p versus h/ε in Figure 2-6; it is worth noting that the curves when plotted in this fashion become independent of the trailing edge clearance ratio ε.

As a final point, when the side gaps of the plate are closed off, r=0, and (2-37) becomes

$$\frac{h}{\varepsilon} = \frac{1}{u} ,$$

or $$hu = \text{constant}.$$

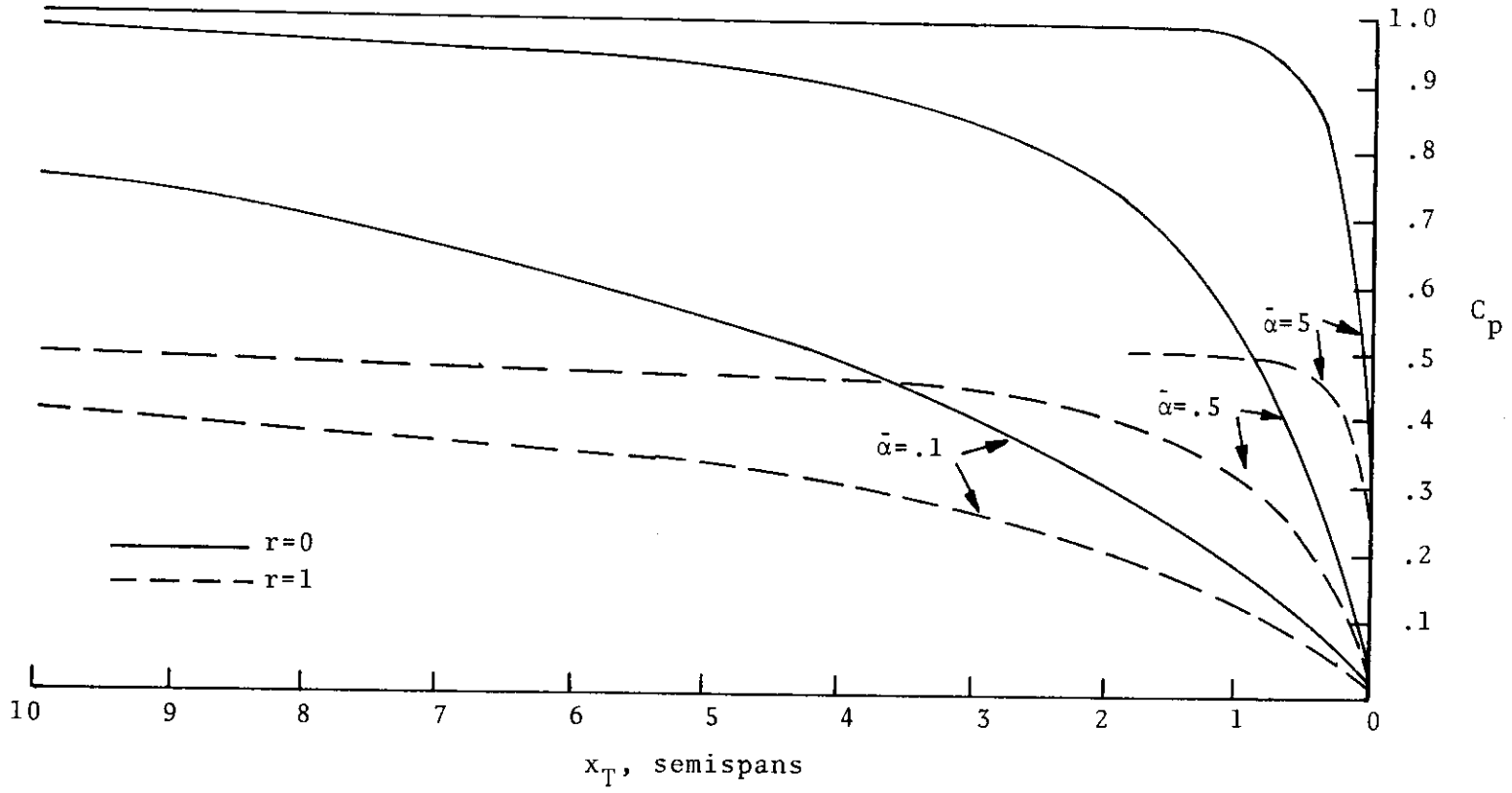

Figure 2-5. Pressure Distribution Given by the Case III Solution. Leading Edge Effects IGNORED. $r = \delta/\alpha$, $\bar{\alpha} = \alpha/\varepsilon$

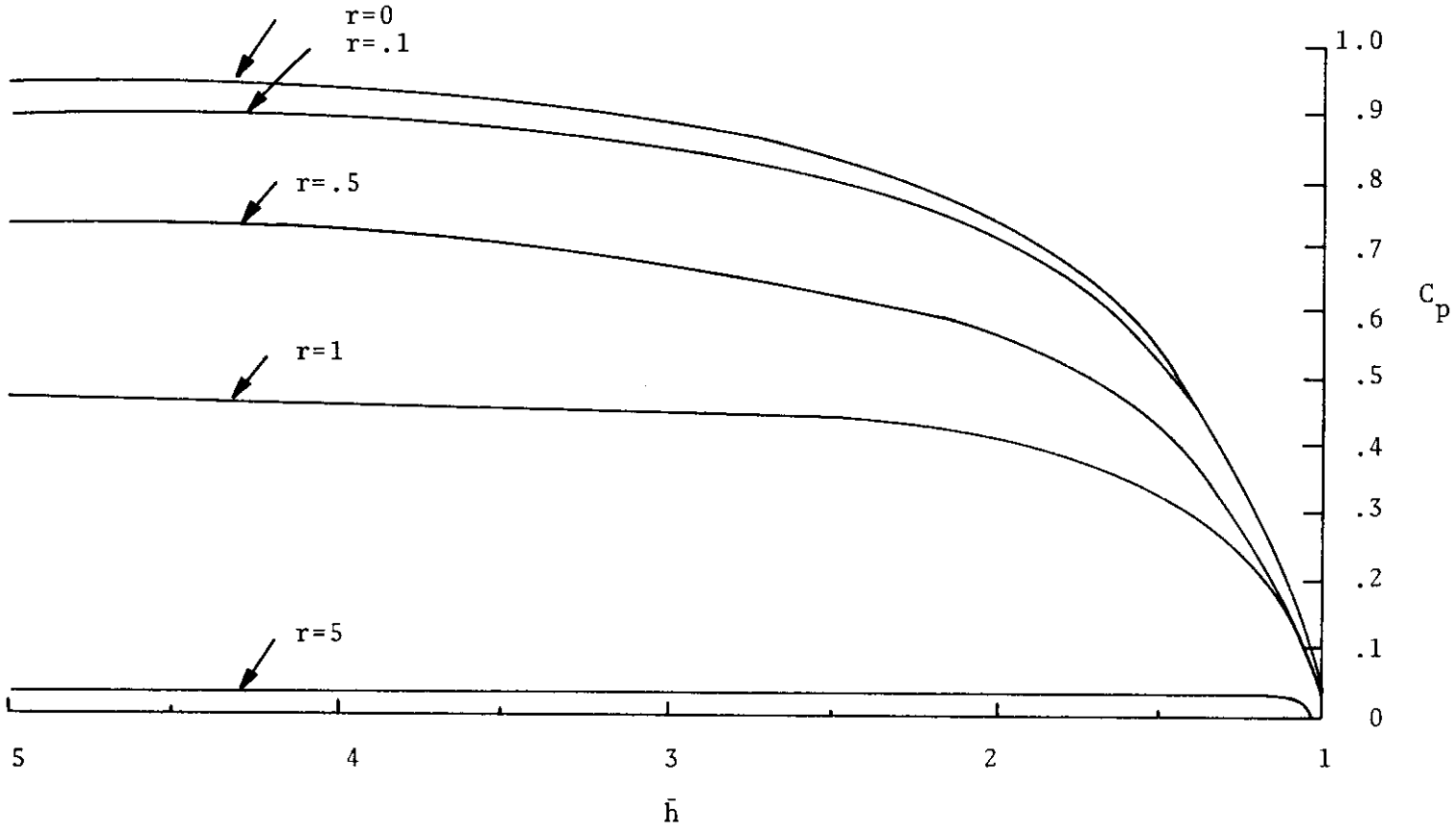

Figure 2-6. Pressure Coefficient Versus Normalized Channel Height Given by the Case III Solution. $r = \delta/\alpha$, $\bar{h}=h/\varepsilon$

This is the equation of one-dimensional incompressible mass continuity.

The form of (2-37) should serve to dim any hopes of finding an analytic solution to equations (2-16). Even though one derivative has been ignored so that only one boundary condition had to be satisfied, the solution appears as a somewhat inconvenient inverse relationship which has no advantage over a simple numerical integration of (2-33) for purposes of calculating the total lift. It is clear that any tractable attempt at a solution satisfying conditions at both the leading and trailing edges must involve either a numerical solution or additional approximations.

2.6 CASE IV - AN APPROXIMATION TO THE COMPLETE EQUATIONS

Although a numerical scheme could be devised to give precise solutions to (16), a separate solution would be required for each set of the geometric parameters α, δ, ε, and c. Giving the variation of the lift and moment with each of these parameters, while eventually useful, could involve an excessive amount of computer time. In this section we propose a linear flow theory which encompasses the major effect of the nonlinear terms, yet gives simple results which fairly clearly show the effect of geometric variations.

In the limit of very large chord, it can be assumed that the pressure over the central portion of the wing will approach the steady state crossplane flow of Case II. Thus, an easy way to satisfy the boundary conditions is to calculate separate solutions for the flow at the leading and trailing edges and to join these to the crossplane flow. At the leading edge, the flow assumes the character of Case I, whereas at the trailing edge, we would expect the result to be very near that of Case III.

For convenience we define the following terms which represent the steady state crossplane flow:

$$u_o \equiv \frac{\delta}{(\alpha^2 + \delta^2)^{1/2}}$$

$$w_o \equiv \frac{\alpha}{(\alpha^2 + \delta^2)^{1/2}}$$

The major deficiency of the potential flow solution of Case I is that for large values of x, it predicts a steady side gap flow w can be maintained without any pressure drop through the gap. That solution is a linearization which assumes that u is everywhere close to the freestream value, whereas it is known from our previous studies that u is less than u_o everywhere except near the trailing edge. Thus, it is logical to linearize about u_o, as follows:

$$u = u_o + u'$$

Thus u_o appears as a parameter and we solve for the new variable u'. When this is substituted into (2-16b) we obtain

$$2\delta A w_x = -2u_o u' + (w_o^2 - u'^2 - w^2) \qquad (2\text{-}40)$$

The last three terms enclosed in parenthesis are all neglected, since it can be shown that w_o^2 is small and comparable to the remaining terms. When (2-16a) is differentiated and (2-40) is substituted into the result, a characteristic equation is produced:

$$u'_{xx} - \frac{\alpha}{h} u'_x - \frac{u_o u'}{Ah} = 0 \qquad (2\text{-}41)$$

This has a solution of the form

$$u' = c_1 e^{\lambda_1 x} + c_2 e^{\lambda_2 x} \qquad (4\text{-}42)$$

where

$$\lambda_{1,2} = \frac{\alpha}{2h} \pm \sqrt{\frac{\alpha^2}{4h^2} + \frac{u_o}{Ah}} \qquad (2\text{-}43)$$

Following the approach taken in Case I, we look for a solution which satisfies a boundary condition at the leading edge and at $x = \infty$. Fow w these become

$$w = 0 \quad \text{at} \quad x = 0$$
$$w = w_o \quad \text{at} \quad x = \infty$$

Thus, $w = w_o (1 - e^{\lambda_2 x})$.

This can be differentiated and put into (2-40) to obtain the solution for u' in the forward region of the wing:

$$u' = \alpha A \lambda_2 e^{\lambda_2 x} \qquad (2\text{-}44)$$

It can be shown that for the case of $\alpha \ll \delta$, this result is consistent with (2-24). The pressure coefficient is most accurately obtained from this result using

$$C_p = 1-(u_o + u')^2. \qquad (2\text{-}45)$$

Computing in this fashion automatically includes both the momentum and side gap effects on the pressure distribution.

At the trailing edge, it is convenient to convert to the trailing edge variable x_T defined in (2-38), and to look for solutions which asymptotically approach the steady state (Case II) solution as $x_T \to \infty$. This is straightforward, we merely reject the solution involving λ_2, which diverges, and use the λ_1 solution which decays exponentially. Using the boundary condition (2-17b) we obtain

$$u' = (1-u_o)\ e^{-\lambda_1 x_T} \qquad (2\text{-}46)$$

There is a minor problem with the variable h, which is treated as a parameter in these solutions but in fact is a function of chordwise position. For small α this is not a problem, we merely set $h=\varepsilon$, whereas in the more practical case of large α we set $h=\varepsilon$ at the trailing edge and $h=\varepsilon+\alpha c$ at the leading edge. The result of these computations is shown in Figure 2-7 for typical geometric parameters. It can be seen that the primary effect of the momentum is to increase the lift at the leading edge and decrease it at the trailing edge. The net effect on the lift is rather small, but a substantial nose-up moment is generated.

The boundary condition we have been using at the trailing edge is valid for the case of a flat plate at a very low angle of attack. For wings with thickness or large α, a more accurate boundary condition can be computed using the methods developed by Barrows,

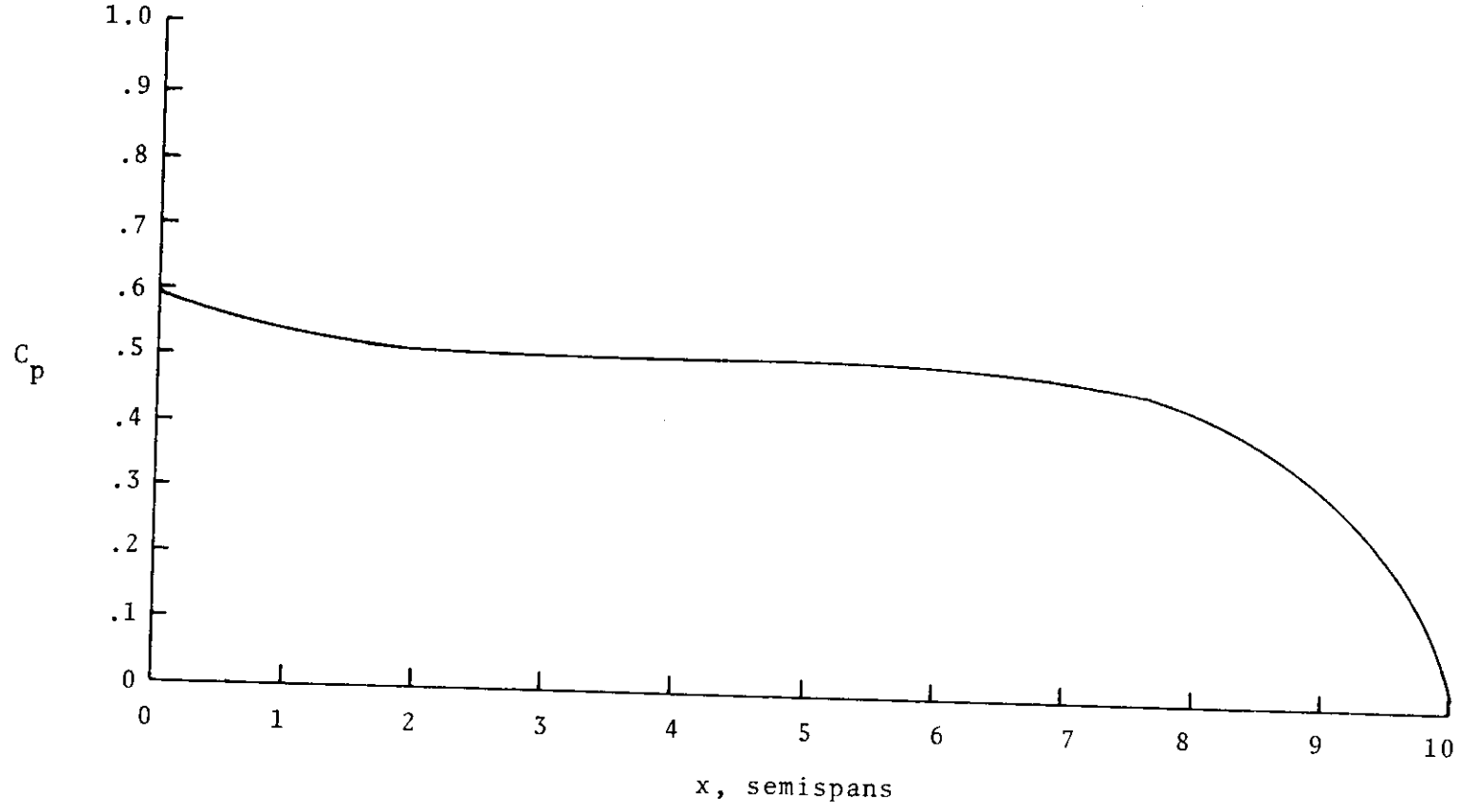

Figure 2-7. Pressure Distribution as Calculated by the Method of Case IV. ε=0.1, $\alpha=\delta=.01$, AR=.2

Widnall, and Richardson (1970). The form of trailing edge solution developed in this section is so simple that it is a perfectly straightforward matter to solve for any pressure condition which may be found, either from analytical or empirical sources.

2.7 CONCLUSIONS TO SECTION 2

An accurate solution for the flow past a ram air cushion must take into account the effects of both momentum and viscosity on the flow out the side gaps. Four solutions have been presented in this chapter, with each succeeding one giving a more accurate solution to the problem posed by the governing equations (2-16). It is clear that this lifting surface cannot be analyzed with classical aerodynamic techniques, yet neither are the methods developed for conventional air cushions adequate for such analysis. The final solution proposed here (Case IV) represents a blend of both technologies and should give a reasonably accurate approximation to the lift and moment acting on the undersurface of a ram air cushion. Greater accuracy and flexibility to analyze more sophisticated configurations will most likely come with the development of proper numerical techniques.

3.0 ANALYTIC SOLUTIONS FOR ASYMMETPICAL FLOW

The basic assumption which led to the simple analyses of the last chapter is that the flow conditions are essentially uniform in each cross sectional plane. Obviously, this must be abandoned in the case of asymmetrical flow if we are to predict such important stability derivatives as roll stiffness and side sway stiffness. In this chapter several solutions are presented for very simple geometric situations which may serve as a basis for comparison with eventual numerical techniques.

3.1 ELLIPTICAL WING

Consider the wing flying in close proximity to the ground at an angle of attack α and a roll angle γ. (Figure 3-1). The case for which $\gamma=0$ was first considered by Widnall and Barrows (1970), who proposed a linear flow theory with the assumption that $\alpha << \varepsilon$. This is retained here, along with the additional assumption that $\gamma << \varepsilon$. The parameter ε used in that reference was defined as the vertical clearance normalized by the wing chord, whereas here we normalize by the semispan in order to preserve consistency with the other chapters. The height h of the channel under the wing is given by

$$h = \varepsilon - \alpha x - \gamma y \tag{3-1}$$

The governing equation for this type of lifting surface problem may be obtained from (2-15) by simply replacing d/dx with ∇, where ∇ is the two-dimensional operator $\vec{i}\,\partial/\partial x + \vec{j}\,\partial/\partial y$. With $u = \nabla\Phi$, we obtain

$$h\nabla^2\Phi + \nabla\Phi\cdot\nabla h = 0. \tag{3-2}$$

This formulation assumes that variations of Φ in the vertical direction are small and may be neglected, but the assumption that Φ is the same throughout each cross-sectional plane is dropped.

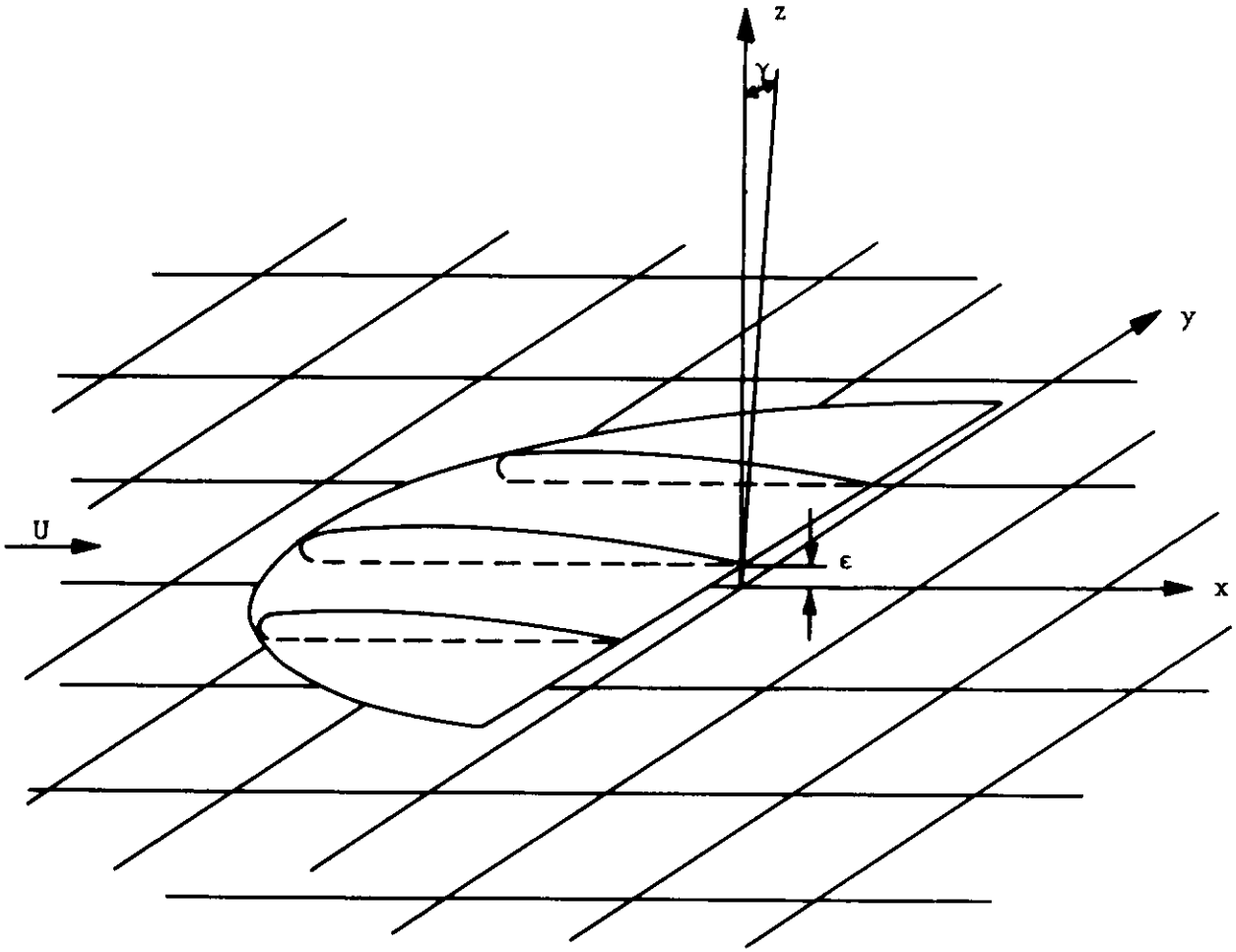

Figure 3-1. Elliptical Wing at a Small Roll Angle in Close Proximity to the Ground

Following the notation of Chapter 2, we use a bar to denote division by ε. Thus (3-1) and (3-2) are written

$$\bar{h} = 1 - \bar{\alpha}x - \bar{\gamma}y \tilde{=} 1, \tag{3-3}$$

$$\nabla^2 \phi \tilde{=} -\nabla\Phi \cdot \nabla\bar{h}. \tag{3-4}$$

An expansion for Φ is written in the following form:

$$\Phi = x + \phi \tag{3-5}$$

$$\phi = \bar{\alpha}\phi_1 + \bar{\gamma}\phi_2 + \bar{\alpha}\bar{\gamma}\phi_3 \tag{3-6}$$

Here x denotes the freestream potential, ϕ_1 is the solution for angle of attack alone, ϕ_2 is a solution for roll angle alone, and ϕ_3 gives the combined effect of roll angle and angle of attack.

When (3-5) and (3-3) are substituted into (3-4) and terms of like order are equated, we obtain governing equations for the individual terms.

$$\nabla^2 \phi_1 = 1, \tag{3-7}$$

$$\nabla^2 \phi_2 = 0 \tag{3-8}$$

$$\nabla^2 \phi_3 = \frac{\partial \phi_1}{\partial y} + y \tag{3-9}$$

Terms of $O(\bar{\alpha}^2)$ or $O(\bar{\gamma}^2)$ or higher are neglected.

The boundary condition at the trailing edge may be obtained from (2-17b):

$$\phi_x = 0 \text{ at } x = 0 \tag{3-10}$$

We also have a condition similar to (2-17a) which states that the velocity perturbation tangent to the leading edge is zero, or in other words the potential is constant along the edge. For convenience, we chose this constant to be zero, so that with the elliptic leading edge shown in Figure 3-3, we obtain

$$\phi = 0 \text{ along } (x/c)^2 + y^2 = 1 \tag{3-11}$$

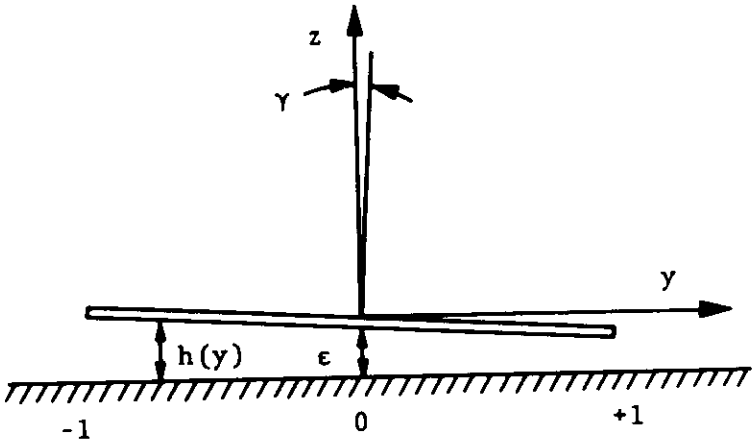

Figure 3-2. Rear View of Elliptical Wing

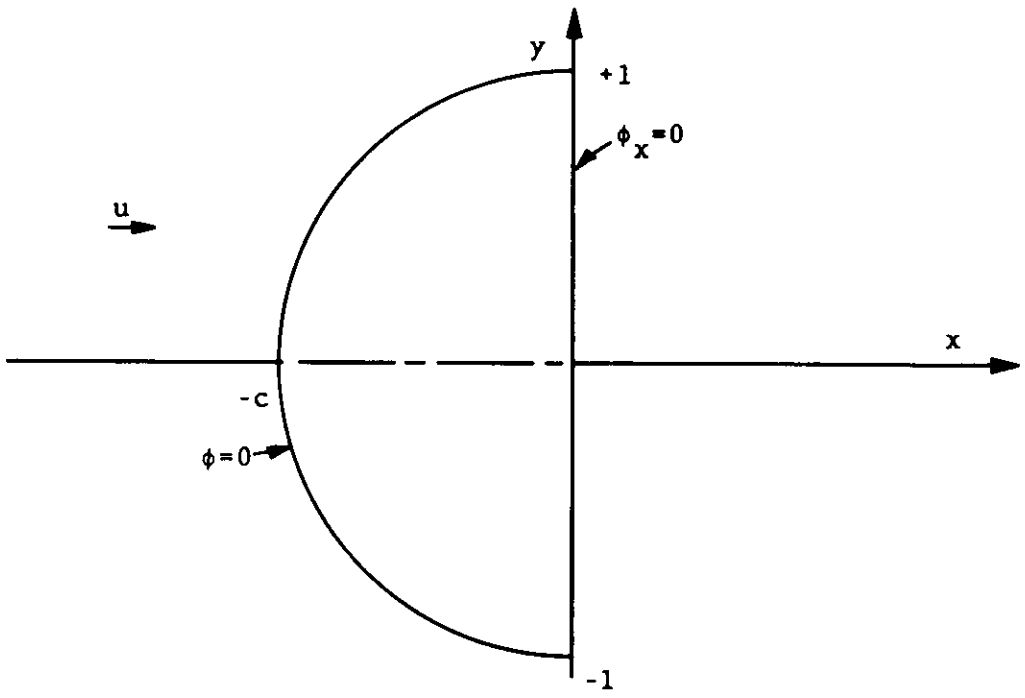

Figure 3-3. Boundary Conditions for the Potential ϕ

Equations (3-10) and (3-11) give a total of six conditions, two for each of the terms ϕ_1, ϕ_2, and ϕ_3.

The solution for ϕ_1 found by Widnall and Barrows (1970) becomes in the present notation

$$\phi_1 = \frac{c^2}{2(c^2+1)} \left[\frac{x^2}{c^2} + y^2 - 1 \right] \tag{3-12}$$

The solution for ϕ_2 is, quite simply, $\phi_2 = 0$. This is certainly logical, for if the angle of attack is zero, there is no way the wing can influence the flow, whatever the roll angle may be.

Finally, the solution for ϕ_3 can be found by a variety of means, the best being trial substitution:

$$\phi_3 = ky\ \phi_1 \ , \tag{3-13}$$

where

$$k \equiv \frac{1+2c^2}{1+3c^2} \tag{3-14}$$

The lift and rolling moment coefficients may readily be computed from

$$C_L = \frac{2}{\text{Area}} \int_{-1}^{+1} \Gamma(y)\ dy \tag{3-15}$$

$$C_\ell = \frac{2}{\text{Area}} \int_{-1}^{+1} y\Gamma(y)\ dy \tag{3-16}$$

Note that the characteristic length used to normalize the moment coefficient is the semispan. Since to $O(\bar{\alpha})$ the potential above the wing is zero, we may use $\Gamma(y) = -\phi(o,y)$. We obtain for the lift

$$C_L = \frac{8\bar{\alpha}}{3\pi} \left(\frac{c}{1+c^2} \right) \tag{3-17}$$

The rolling moment is best expressed as follows:

$$C_{\ell} = - \frac{k\bar{\gamma}}{5} C_L \qquad (3\text{-}18)$$

This shows that the rolling moment is proportional to the product of the lift and the roll angle, and is inversely proportional to ϵ. The limiting values for k as given by (3-14) are of some interest:

As $c \to o$, $k \to 1$ (high aspect ratio).
As $c \to \infty$, $k \to 2/3$ (low aspect ratio).
For $c=1$, $k=3/4$ (semicircular wing).

The magnitude of this rolling moment may be judged by considering the lift to be composed of two components, one on each side of the wing, as shown in Figure 3-4. For no roll, each semispan has half the lift. Consider the case of large aspect ratio, so that k=1 in (3-18). The maximum roll angle occurs when one tip of the wing touches the ground, so that $\bar{\gamma}$ also equals 1. The proper moment as given by (3-18) is reproduced if we increase the lift on one side by 40% and decrease it by 40% on the other side. Therefore, this wing will have roughly the same roll characteristics as two conventional air cushions, each acting at the mid point of one semispan and supporting half the weight, in which the maximum force capability of each cushion is 40% greater than its equilibrium load. This may be overextending the theory slightly, since it is assumed that $\bar{\gamma} << 1$, but for small roll angles the two situations should be analogous. If we have a very low aspect ratio wing, the roll torque will be only 2/3 of that given by the analogy. However, in that case, we must remember that the solution calculated here only gives the forces due to momentum effects, and does not include the "cushion" lift (see Chapter 2), which will produce its own roll torque.

As of this writing, there are no known analytic solutions which include both the momentum and cushion effects, and it appears that the best approach to this type of calculation is to use a numerical

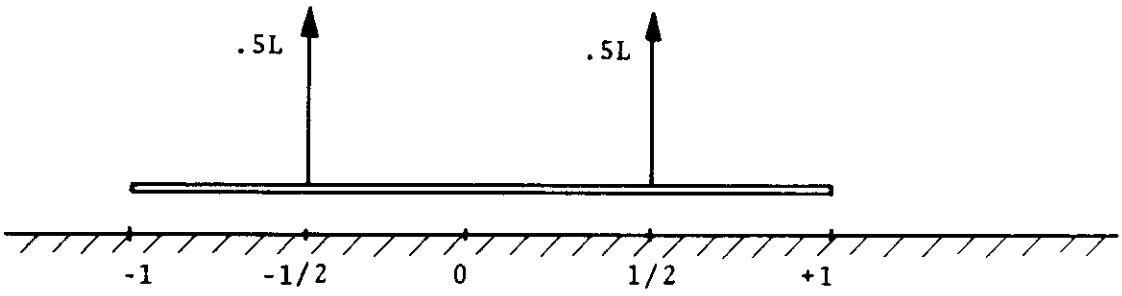

(a) Equilibrium case, $\bar{\gamma} = 0$

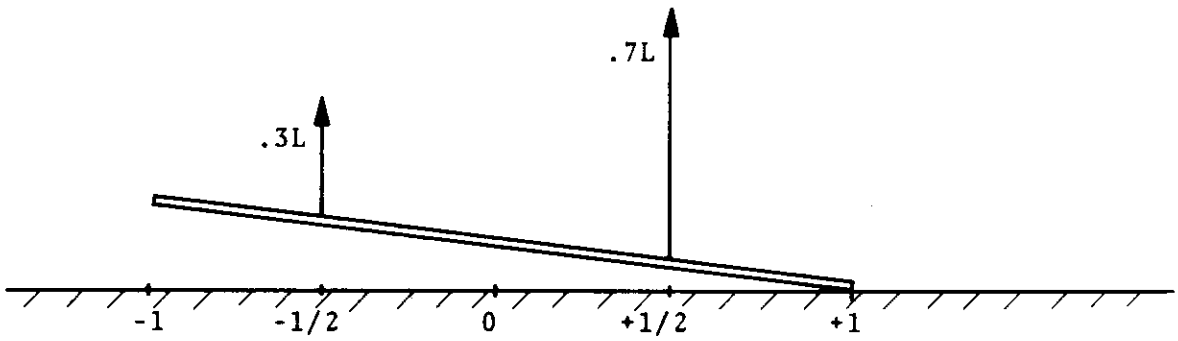

(b) Maximum roll case, $\bar{\gamma} = 1$

Figure 3-4. Effect of Roll on the Lift Distribution for a Wing of High Aspect Ratio

computer technique. The solution just cited does serve to illustrate the statement made in Chapter 1 that the pressure may vary significantly from one region of the wing (cushion) to the next, even though no separating barrier exists between them.

3.2 RECTANGULAR WING WITHOUT SIDE GAPS

A flat plate in a rectangular channel, of course, holds a somewhat greater interest than the previous example for the problem of tracked vehicles. The situation shown in Figure 3-5, in which there is no gap between the sides of the plate and the channel, is amenable to analytic treatment and hence serves as an interesting limiting case. The initial formulation and governing equations are identical to those of the previous section, with the only difference being the nature of the boundary conditions. The leading and trailing edge conditions are the same, except for the geometry, but there is a new condition of no flow through the side edges, $\phi_y=0$ at $y=\pm 1$.

For the case of no roll, the flow past this wing becomes two-dimensional and we end up with the simple result of Widnall and Barrows (1970) for the first order solution:

$$\phi_1 = (x^2-c^2)/2 \tag{3-19}$$

The governing equation for ϕ_3 thus becomes, from (3-9),

$$\nabla^2 \phi_3 = y. \tag{3-20}$$

A particular solution which satisfies this and the side edge boundary condition is

$$\phi_3{}^p = (y^3-3y)/6. \tag{3-21}$$

This, however, does not satisfy the leading edge condition. To do this, we propose a homogeneous solution $\phi_3{}^h$ which satisfies Laplace's equation and is equal to $-\phi_3{}^p$ at the leading edge. For convenience, we let

$$\phi_3{}^h = \phi \tag{3-22}$$

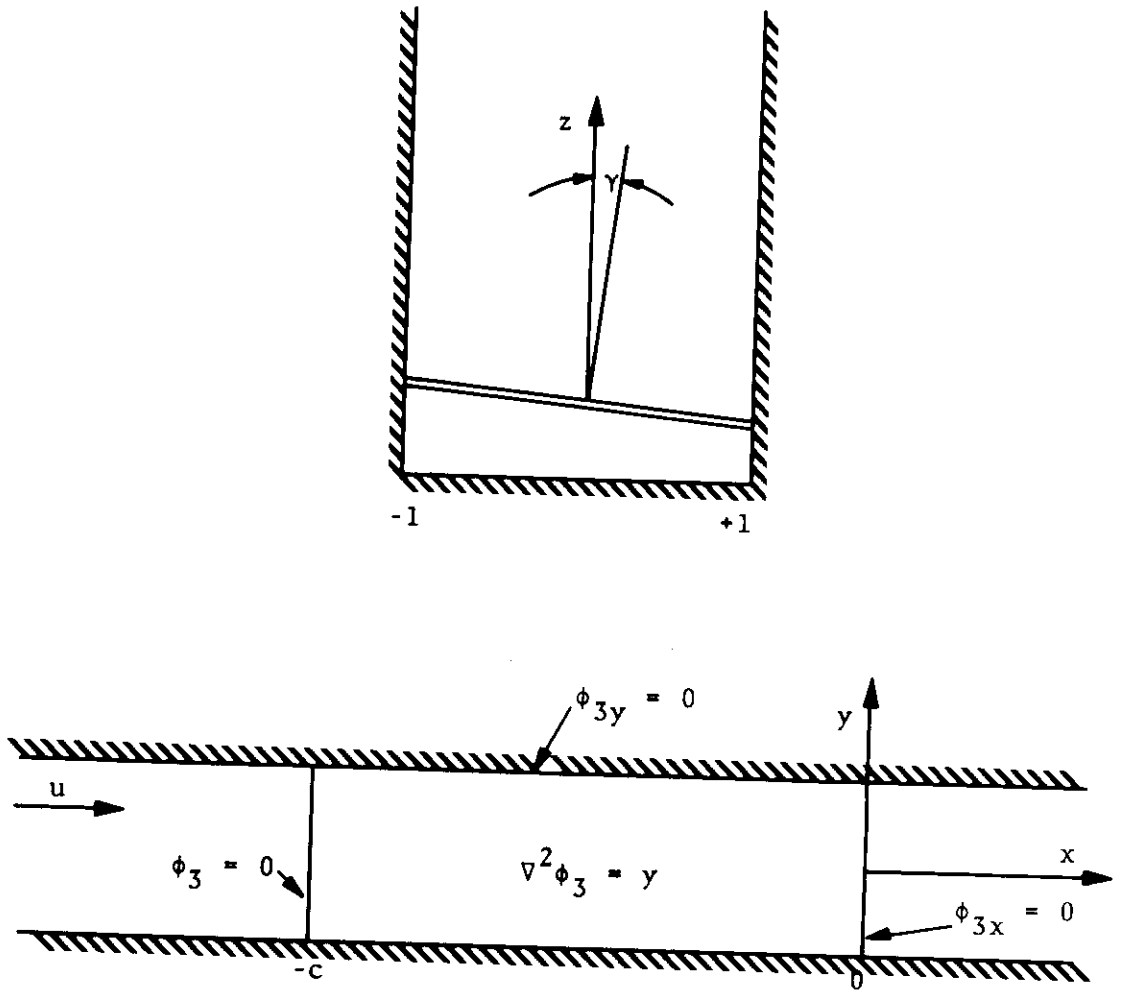

Figure 3-5. Flat Plate in a Rectangular Trough Without Side Gaps. Boundary Conditions for Antisymmetric Component of Flow

The complete equations and boundary conditions on ϕ become

$$\nabla^2\phi=0 \tag{3-23}$$

$$\phi_x=0 \text{ at } x=0 \tag{3-24}$$

$$\phi_y=0 \text{ at } y=\pm 1 \tag{3-25}$$

$$\phi= (3y-y^3)/6 \text{ at } x=-c \tag{3-26}$$

This is solved using a series solution and separation of variables:

$$\phi = \sum_{1}^{\infty} A_n \cosh \frac{n\pi x}{2} \sin \frac{n\pi y}{2} \tag{3-27}$$

Notice that the series when written in this fashion automatically satisfies (3-23) and (3-24), whereas (3-25) is satisfied for all odd n. The problem is thus reduced to that of choosing the A_n to satisfy (3-26), which is most conveniently done by differentiating (3-26) and (3-27) with respect to y, setting x=-c, and equating the results:

$$1-y^2 = \pi \sum n A_n \cosh \frac{n\pi c}{2} \cos \frac{n\pi y}{2} \tag{3-28}$$

This is solved by the standard Fourier method of multiplying by cos $m\pi y/2$, integrating, and using the orthogonality of the cosine function. The result for odd n becomes

$$A_n = \frac{32(-1)^{\frac{n-1}{2}}}{n^4\pi^4 \cosh(n\pi c/2)}$$

Since the A_n drop off as n^{-4}, the series converges extremely rapidly. With only one term, the series in (3-28) has a maximum error of less than 4%, so that it is probably not worthwhile to include any additional terms. Thus, when we add $\phi_3{}^p$ and $\phi_3{}^h$ we obtain

$$\phi_3 = \frac{y^3-3y}{6} + \frac{32 \cosh(\pi x/2)\sin(\pi y/2)}{\pi^4 \cosh(\pi c/2)}$$

The pressure coefficient can be computed from this as in (3-25) by differentiating with respect to x, which shows that all the pressure variation comes from the second term and is concentrated in the forward portion of the wing. The rolling moment coefficient may be computed using (3-16). For the case of large chord, the homogeneous term becomes negligable at x=0 and we obtain

$$C_\ell = -\frac{4\bar{\alpha}\bar{\gamma}}{15c} \qquad (3\text{-}29)$$

The rolling moment, being a momentum effect, approaches a fixed asymptotic value as $c\to\infty$ and does not increase with the total area of the lifting surface. Thus, the moment coefficient based on planform area decreases like c^{-1}, as shown, which may be a problem for very long vehicles whose roll stiffness requirements may be expected to be proportional to their size, and hence their length if the width is fixed. These comments apply to both (3-18) and (3-29). Thus for such large vehicles some type of device such as a ventral fin will probably be needed to increase the roll stiffness.

3.3 TREFFTZ PLAN FLOW FOR RECTANGULAR WING WITH SIDE GAPS

This problem has been solved in (A) for the case of $\gamma=0$, using the method of matched asymptotic expansions. Here we present a modification of that solution which allows for a small roll angle, Figure 3-6. For mathematical simplicity we analyze the equivalent problem shown in Figure 3-7.

The horizontal velocity for the channel flow in the symmetrical case with unit downwash is obtained from mass continuity:

$$v = \frac{y}{h} \qquad (3\text{-}30)$$

This holds throughout the channel region, i.e., everywhere under the wing except near the edges, where the flow becomes two-dimensional. When there is a finite roll angle h becomes a function of y,

$$h = \varepsilon - \gamma y.$$

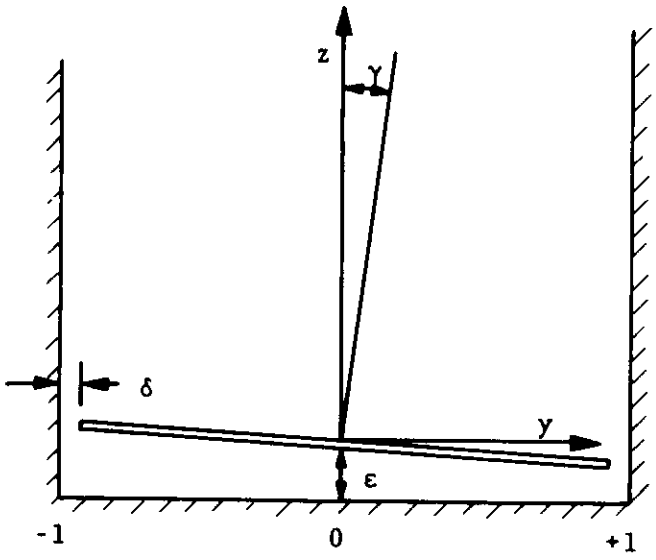

Figure 3-6. Trefftz Plane of a Wing in a Rectangular Trough with Side Gaps

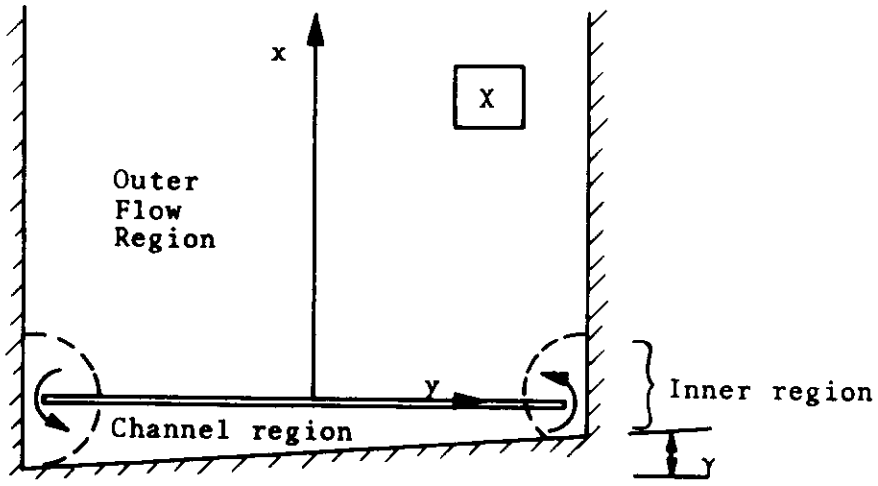

Figure 3-7. Equivalent Problem Under Consideration

In the asymmetrical case, if $\gamma \ll \varepsilon$, an approximation which gives the functional relation between v and y may be made as follows:

$$v \sim \frac{y}{\varepsilon - \gamma y} \cong \frac{y + \gamma \bar{y}^2}{\varepsilon} \tag{3-31}$$

This differs from the actual relation by a constant for points in the channel region.

In order to represent the solution at the side edges we note that in the limit of vanishingly small gap the flow approaches that of an ideal sink. A simple sink with a potential of the form ln X, where $X = y+iz$, cannot be used since it allows flow through the ground plane. To avoid this difficulty we use an infinite series of sinks of the form

$$S(X) = -\frac{2}{\pi} \ln \sinh \frac{\pi X}{2\varepsilon} \tag{3-32}$$

The complex velocity $q = v-iw$ for this potential is given by

$$S'(X) = \frac{dS}{dX} = \frac{-1}{\varepsilon} \coth \frac{\pi X}{2\varepsilon} \tag{3-33}$$

For points on the wing we set $z=0$ and obtain $X=y$. If $y > \varepsilon$, the sink velocity as given by (3-33) very quickly approaches the asymptotic limit for $y=\infty$.

$v \to \frac{+1}{\varepsilon}$ for points to the left of the sink

$v \to \frac{-1}{\varepsilon}$ for points to the right of the sink

$v=0$ for points at the horizontal location of the sink

Also note that the vertical velocity w for this function is zero for all lines $z=n\varepsilon$, $n=0, \pm 1, \pm 2, \ldots$

The velocity in the channel region may be written as follows:

$$q^c = i + \frac{X+\bar{\gamma}X^2}{\epsilon} + v_o + (1-m)\, S'(X+1) + (1+m)S'(X-1) \tag{3-34}$$

The first term in this expression represents the uniform downwash flow across the wing. The second term represents the horizontal velocity component as given by (3-31). The third term is a constant added to maintain the condition of no flow through the walls of the trough. Finally, the last two terms are added to represent the outflow through the side gaps, located at $X=\pm 1$. Notice that these sink terms contain a common symmetrical component of magnitude one, plus equal and opposite components of magnitude m. With no roll m=0. The problem consists of determining the relationship between m and the roll angle γ.

The symmetrical aspect of the problem is not of interest here, so we subtract all such terms in (3-32) and retain only those elements caused by the roll angle. We use the subscript 3 for this portion to maintain consistency with the other sections of this chapter.

$$q_3^c = v_o + \frac{\bar{\gamma}X^2}{\epsilon} - mS'(X+1) + mS'(X-1) \tag{3-35}$$

We now apply the boundary condition that there is no flow through the right wall of the trough. Setting z=0, y=1, and taking the real part of (3-35) we obtain

$$v = v_o + \frac{\bar{\gamma}+m}{\epsilon} = 0 \tag{3-36}$$

or

$$v_o = -\frac{\bar{\gamma}-m}{\epsilon}$$

The potential is found by integrating (3-35) and taking the real part

$$\phi_3^c = v_o y + \frac{\bar{\gamma} y^3}{3\epsilon} - mS(y+1) + mS(y-1) \qquad (3\text{-}37)$$

3.3.1 Edge Flow Region

As in the symmetrical flow case, we magnify the right edge of the wing tip to obtain an inner region as shown in Figure 3-8. We define a right edge outer variable

$$y_r = y-1, \qquad (3\text{-}38)$$

and an inner variable

$$\tilde{y}_r = y_r/\delta.$$

The potential for the flow in Figure 3-8 is quite well known:

$$\phi_3^i = \frac{2m}{\pi}\left[\pm \ln\left(y_r + \sqrt{\tilde{y}_r - 1}\right) + c^i\right]$$

This function has a branch cut along the surface of the wing. The outer limit is obtained by letting $\tilde{y}_r \to \infty$, converting to the outer variable, and taking the + sign since this represents the wing upper surface,

$$\phi_3^{io} = + \frac{2m}{\pi}\left[\ln \frac{2y_r}{\delta} + c^i\right] . \qquad (3\text{-}39)$$

The channel flow limit is obtained on the lower surface, which means we use the - sign:

$$\phi_3^{ic} = - \frac{2m}{\pi}\left[\ln \frac{2y_r}{\delta} - c^i\right] \qquad (3\text{-}40)$$

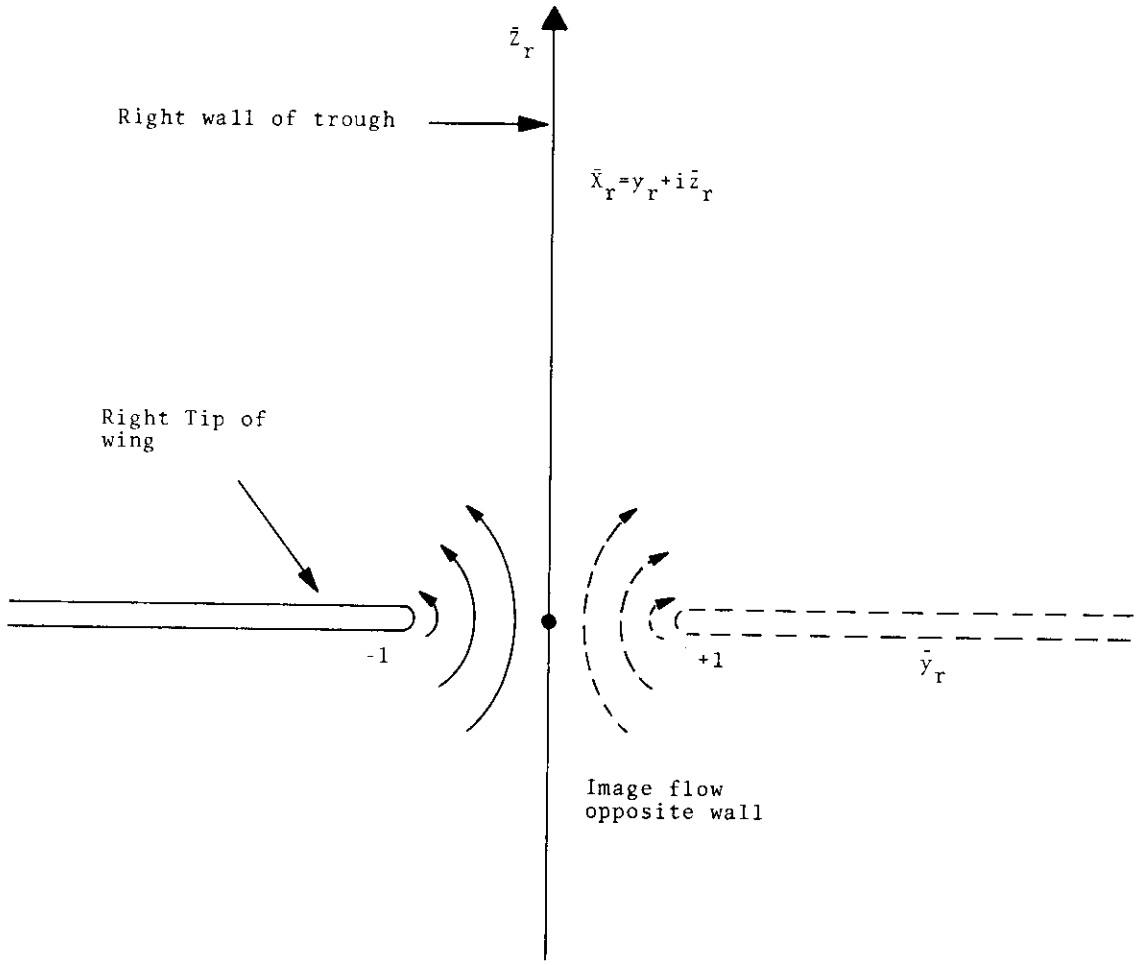

Figure 3-8. Flow in the Inner Region of the Right Wing Tip

3.3.2 Outer Flow Region

The outer flow above the wing may be represented by an alternating series of sources and sinks propagating in the horizontal direction, which satisfies the condition of no flow through the walls of the trough, Figure 3-9. With sufficient experimentation with various trigonometric singularities, it is found that the following complex potential fits the description:

$$\phi_3^o + i\psi_3^o = \frac{2m}{\pi} \ln \tan \frac{\pi(X-1)}{4} \tag{3-41}$$

The inner limit of this may be found for purposes of matching with the edge flow region by using (3-38) and taking the limit as $y_r \to 0$

$$\phi_3^{oi} = \frac{2m}{\pi} \ln \frac{\pi y_r}{4} \tag{3-42}$$

By comparing this to (3-39) we have

$$c^i = \ln \frac{\pi\delta}{8} , \tag{3-43}$$

which completes the matching above the wing. Below the wing the matching proceeds in a similar fashion, using (3-36) and (3-38) in (3-37), and letting $y_r \to 0$ to get the inner limit of the channel flow solution:

$$\phi_3^{ci} = -\frac{\bar{\gamma}+m}{\epsilon} - \frac{\bar{\gamma}}{3\epsilon} - \frac{2m}{\pi} \ln \frac{\pi y_r}{\epsilon}$$

Using (3-40) and (3-43) we have

$$\phi_3^{ic} = -\frac{2m}{\pi} \left[\ln \frac{\pi y_r}{\epsilon} + \ln \frac{16\epsilon}{\pi^2\delta^2} \right]$$

By setting $\phi^{ci} = \phi^{ic}$ we can solve for m:

$$m = \frac{2\bar{\gamma}}{3 + \frac{6\epsilon}{\pi} \ln \frac{16}{\pi^2\delta^2}} \tag{3-44}$$

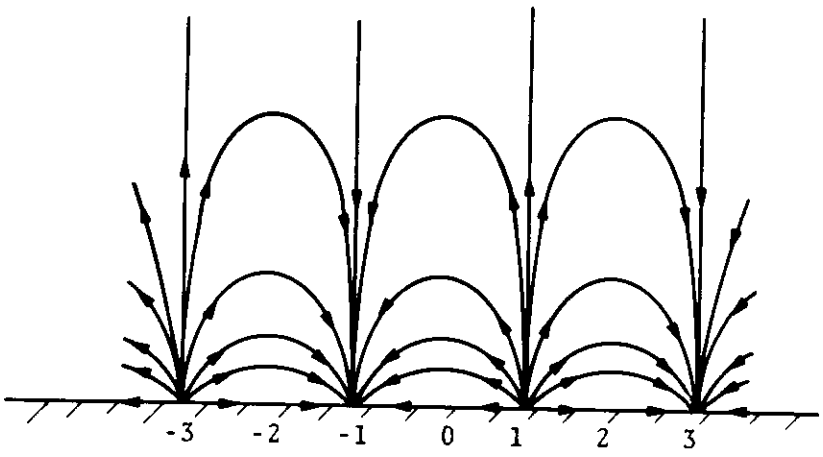

Figure 3-9. Outer Flow Pattern for the Antisymmetric Component of the Problem Shown in Figure 3-7

This formula shows that as the side gap $\delta \to 0$, the differential mass flux m also becomes zero, but not very rapidly.

The rolling moment coefficient may be obtained by applying (3-16) in the same manner as before, using (3-37). We obtain

$$C_\ell = \frac{-8\bar{\gamma} + 10m}{15\varepsilon c} \qquad (3\text{-}45)$$

As with the elliptical wing the result is best expressed as a percentage of the momentum lift coefficient. The resulting formulas are quite cumbersome unless certain simplifications are introduced. Let us define

$$D \equiv \frac{2\varepsilon}{\pi} \ln \frac{4\varepsilon}{\pi^2 \delta^2}$$

Equation (3-44) can be written

$$m = \frac{2\bar{\gamma}}{3} \left[\frac{1}{1+D+O(\varepsilon)}\right]$$

Even if $\delta << 1$, D is typically quite small. For example, if $\varepsilon=.1$ and $\delta=.01$, D=.38. This allows us to write

$$m \cong \frac{2\bar{\gamma}}{3} (1-D). \tag{3-46}$$

The rolling moment coefficient becomes

$$C_\ell = - \frac{\bar{\gamma}(4+20D)}{45\varepsilon c}$$

The lift coefficient may easily be obtained from the formulas developed in (A)

$$C_L = \frac{2+6D}{3\varepsilon c} \quad ,$$

and ratio of these expressions becomes

$$\frac{C_\ell}{C_L} = - \frac{2\bar{\gamma}}{15} \frac{(1+5D)}{(1+3D)} \tag{3-47}$$

It is worth noting that if $\delta=0(\varepsilon)$, then D may be neglected and the rolling moment becomes identical to that predicted by (3-18) for the case of a very low aspect ratio ellipse. This is to be expected since the side gaps must be an order of magnitude smaller than ε in order to have a significant influence on the potential flow. Recall also that the Trefftz plane of Figure 3-6 makes no assumption about the planform of the wing, the only stipulation being that a uniform downwash is created along the entire span. In the case of extremely small δ it must be remembered that the approximation given by (3-46) is not valid.

4.0 RECOMMENDATIONS FOR FUTURE RESEARCH

The ram air cushion program outlined by Barrows (1971) is reproduced here in Figure 4-1 in order to give a broad overview of the total research picture. Most of the recommendations made in that reference are still valid and particular attention is called to the discussion on active suspension which this author feels may provide a very fertile new area for high speed suspension research. The main purpose to this present chapter is to point out the manner in which the emphasis has changed to different aspects of the program over the past year.

Major advances have been achieved in the first element of Figure 4-1; determining a theoretical flow model. Progress is also well advanced in the model glide tests which have provided a convincing demonstration of the feasibility of the concept. However, the greatest gap in the technical progress of the program is in obtaining good experimental data which can be used to validate the theory, particularly for the lateral stability derivatives. (It is felt at this stage that the longitudinal derivatives are comparatively well understood.) The towing tank tests reported by Boccadoro (1972) represent an excellent start in closing this gap and future efforts will concentrate on refining this experimental technique and obtaining reliable estimates of the stability derivatives. Once this is done a meaningful analysis can be made of the lateral dynamic response to guideway irregularities and crosswind gusts, and the aerodynamic undersurfaces of a ram air cushion vehicle can be defined according to a systematic design procedure.

One area which deserves a good deal of emphasis is the civil engineering aspect of designing a guideway to stringent tolerances. It is stipulated that a major advantage of the ram air cushion is the fact it does not require the entire guideway surface to be smoothly aligned, only the path which the edges of the cushion follow. Most observers agree that this may result in a substantial savings in construction cost but as yet there is no way to quantify

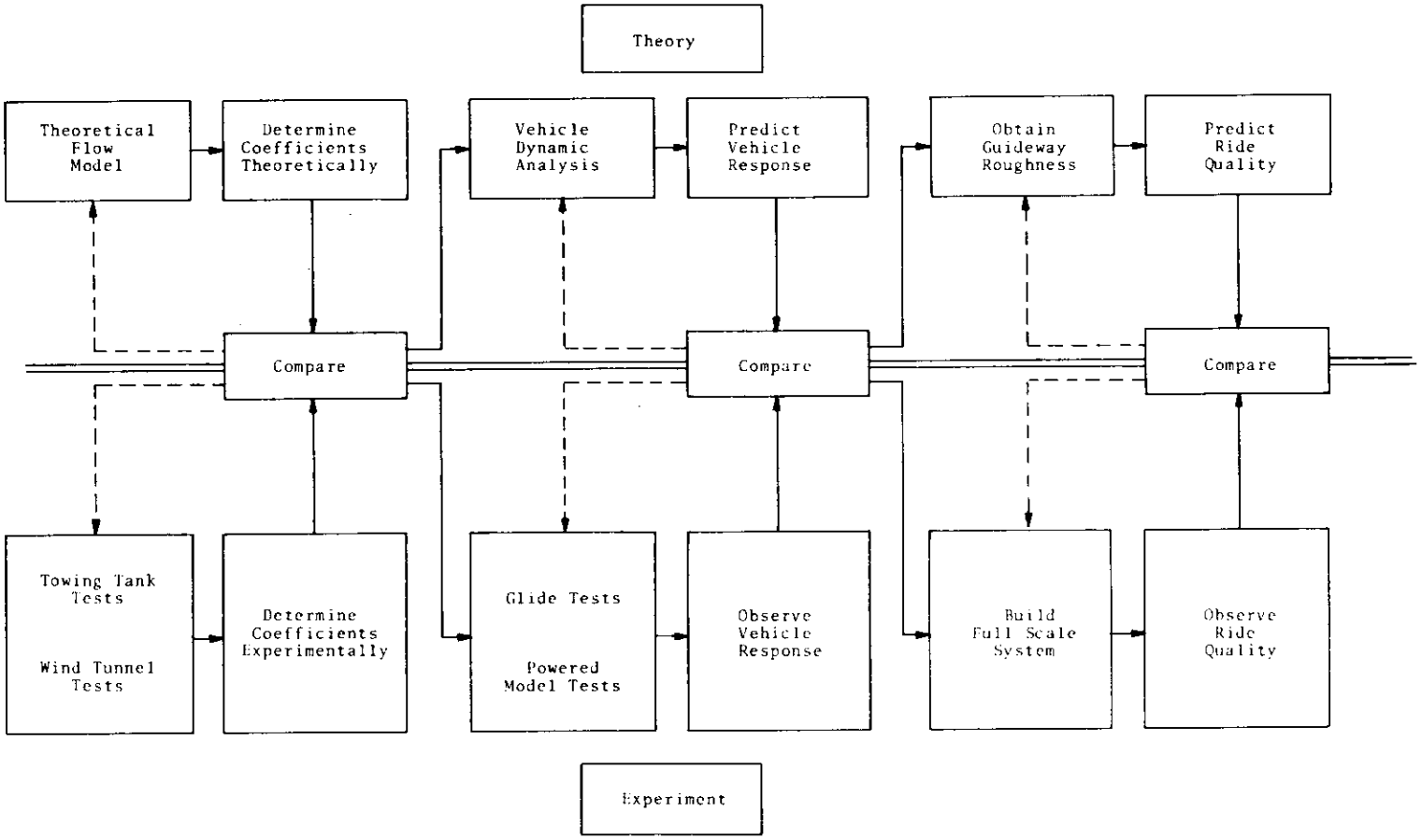

Figure 4-1. Ram Air Cushion Development Program

this advantage so as to provide a meaningful comparison with other concepts for high speed ground transportation. Perhaps research in this area should consist of actually constructing several sample lengths of full scale guideway according to different alignment constraints and observing both the difficulties of fabrication and the irregularities which develop with the passage of time. This would provide first hand information on what is generally conceded to be the most significant aspect of any ground transportation system - guideway cost.

One aspect of the program which is being de-emphasized is the optimization of the dynamic charasteristics of the vehicle-guideway cross-section. Although there are aspects of this problem which maintain a primary importance, such as the precise manner in which the edges of the cushion interface with the guideway, it appears at this point that a rectangular channel represents the best design on which to focus future efforts. There might conceivably be some marginal advantage from a dynamic standpoint of a different configuration but it must be remembered that this is the chosen shape for the TACRV guideway which will be 22 miles long when completed. It is unlikely that any such advantage could warrant a major change in this guideway in the event that a full scale ram air cushion vehicle is built. Experience from such a full scale system would undoubtedly provide the most persuasive information on whether an improvement could be made over the channel configuration, so it does not seem prudent at this stage to expend a significant effort looking for theoretical alternatives.

In closing, it is re-emphasized that the primary purpose of this report is to demonstrate that the dynamic ram air cushion concept represents a logical step forward in the design of a fluid suspension system, rather than a radical departure from conventional air cushion technology. Significant improvements in terms of reduced power requirements, noise, vehicle weight, and guideway construction costs can result from taking advantage of the incoming momentum of the airstream which surrounds any high speed vehicle. The extent of these advantages undoubtedly depends more on the ingenuity of the designer than on any inherent limitation of the principle.

REFERENCES

The notation (A) in the text refers to Barrows (1971).

Barrows, T., (1971) "Progress on the Ram Wing Concept with Emphasis on Lateral Dynamics" PB 210 743.

Barrows, T., and Widnall, S. (1970) "Optimum Lift-Drag Ratio for a Ram Wing Tube Vehicle" AIAA Journal Vol. 8, No. 3.

Barrows, T., Widnall, S.E., and Richardson, H., (1970) "The Use of Aerodynamic Lift for Application To High Speed Ground Transportation", PB 197 242.

Boccadoro, Y. (1972) "Towing Tank Test on a Ram Wing in a Rectangular Channel" to be published by the Transportation Systems Center, Kendall Sq., Cambridge, Mass.

Davis, J. (1972) "Non-Planar Wings in Non-Planar Ground Effect" Ph. D. Thesis, Cal. Inst. of Tech., Pasadena, Cal.

Gray, F.B. (1971) "The Use of Aerodynamic Lift For Suppport of High Speed Surface Transport Vehicles" M.S. Thesis, Ohio State University.

Pepin, J., Widnall, S.E., and Barrows, T. (1971) "An Experimental Study of a Flat-Bottomed Semi-Circular Wing in Very Close Proximity to the Ground" PB 203 602.

Widnall, S.E., and Barrows, T.M., (1970) "An Analytic Solution for Two- and Three-Dimensional Wings in Ground Effect" Journal of Fluid Mechanics, Vol. 41, p. 769.

Gallington, R.W., Miller, M.K., and Smith, W.P. (1972) "The Ram Wing Surface Effect Vehicle" Hovering Craft and Hydrofoil Vol. 11, No. 5.

Giraud, F.L. (1969) "A Preliminary Design Study of a Tracked Air Cushion Research Vehicle" PB 183 319.

Note: Reports with PB prefixes can be obtained from the National Technical Information Service (NTIS), Springfield, Virginia 22151.